# FRACTURE MECHANICS STUDY ON 155 MM M107E1 PROJECTILE MADE FROM ISOTHERMALLY TRANSFORMED HF-1 STEEL

FRANKFORD ARSENAL

FEBRUARY 1976

AD

FA-TR-76015

# FRACTURE MECHANICS STUDY ON 155 MM M107E1 PROJECTILE MADE FROM ISOTHERMALLY TRANSFORMED HF-1 STEEL



February 1976



Approved for public release; distribution unlimited.

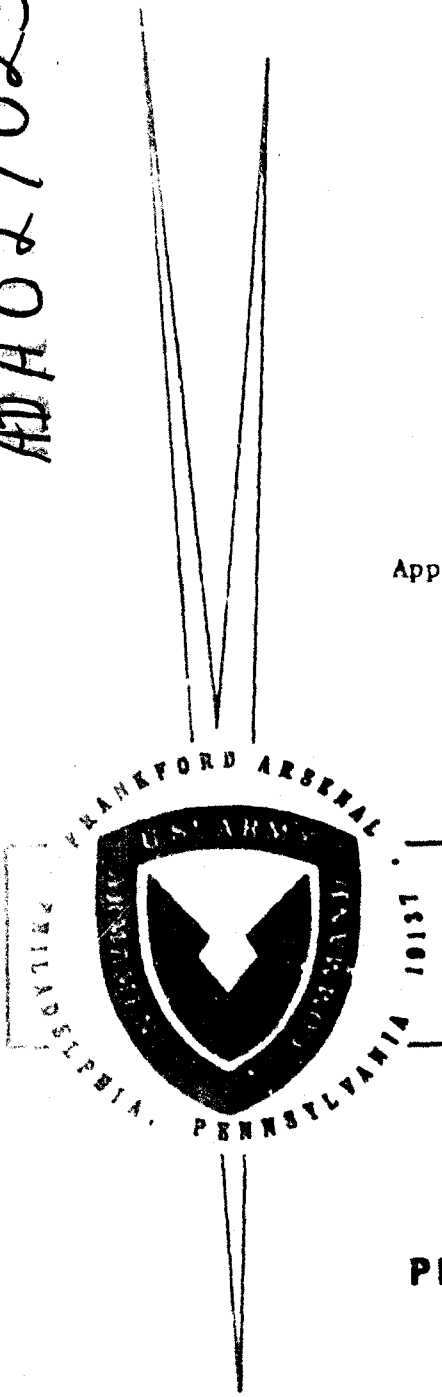


Pitman - Dunn Laboratory

U.S. ARMY ARMAMENT COMMAND
FRANKFORD ARSENAL
PHILADELPHIA, PENNSYLVANIA 19137

## DISPOSITION INSTRUCTIONS

Destroy this report when it is no longer needed. Do not return it to the originator.

The findings in this report are not to be construed as an official Department of the Army position unless so designated by other authorized documents.

UNCLASSIFIED

SECURITY CLASSIFICATION OF THIS PAGE (When Data Entered)

| REPORT DOCUMENTATION PAGE | | READ INSTRUCTIONS BEFORE COMPLETING FORM |
|---|---|---|
| 1. REPORT NUMBER<br>FA-TR-76015 | 2. GOVT ACCESSION NO. | 3. RECIPIENT'S CATALOG NUMBER |
| 4. TITLE (and Subtitle)<br>FRACTURE MECHANICS STUDY ON 155 MM M107 PROJECTILE MADE FROM ISOTHERMALLY TRANSFORMED HF-1 STEEL | | 5. TYPE OF REPORT & PERIOD COVERED<br>Technical Research Report<br>6. PERFORMING ORG. REPORT NUMBER |
| 7. AUTHOR(s)<br>Joseph H. Mulherin<br>William B. Steward<br>John D. Corrie | | 8. CONTRACT OR GRANT NUMBER(s) |
| 9. PERFORMING ORGANIZATION NAME AND ADDRESS<br>Frankford Arsenal<br>Attn: SARFA-PDM<br>Philadelphia, PA 19137 | | 10. PROGRAM ELEMENT, PROJECT, TASK AREA & WORK UNIT NUMBERS |
| 11. CONTROLLING OFFICE NAME AND ADDRESS<br>US Army Armament Command<br>SARRI-LE<br>Rock Island, IL 61021 | | 12. REPORT DATE<br>February 1976<br>13. NUMBER OF PAGES<br>52 |
| 14 MONITORING AGENCY NAME & ADDRESS(if different from Controlling Office) | | 15 SECURITY CLASS. (of this report)<br>UNCLASSIFIED<br>15a. DECLASSIFICATION/DOWNGRADING SCHEDULE<br>NA |

16. DISTRIBUTION STATEMENT (of this Report)

Approved for public release; distribution unlimited.

17. DISTRIBUTION STATEMENT (of the abstract entered in Block 20, if different from Report)

18. SUPPLEMENTARY NOTES

19. KEY WORDS (Continue on reverse side if necessary and identify by block number)

Critical Flaw Sizes
Fracture Mechanics
Artillery Projectile
HF-1 Steel

20. ABSTRACT (Continue on reverse side if necessary and identify by block number)

A linear elastic fracture mechanics approach is used to describe critical flaw sizes in the 155 mm M107E1 HE projectile as manufactured from isothermally transformed HF-1 steel. Based on dynamic fracture toughness determinations and both experimental and analytical determinations of stress, critical crack sizes are calculated for each of the major sources of stress encountered during rough handling (drop testing) and launch. (cont)

DD FORM 1 JAN 73 1473 EDITION OF 1 NOV 65 IS OBSOLETE

UNCLASSIFIED

SECURITY CLASSIFICATION OF THIS PAGE (When Data Entered)

20. ABSTRACT (cont)

Drop tests of intentionally pre-flawed projectiles are used to check the validity of the approach. The low fracture toughness of isothermally transformed HF-1 at -65 degrees F and the relatively high stresses encountered by the projectile (particularly under drop test conditions) result in critical crack depths as small as 0.010 inch. A recommendation is made that isothermally transformed HF-1 not be considered for use in ar HE projectile of the M107 configuration.

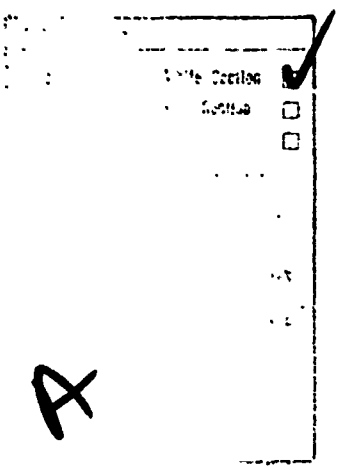



A

## TABLE OF CONTENTS

## LIST OF TABLES



## LIST OF ILLUSTRATIONS

LIST OF ILLUSTRATIONS (Cont)

## INTRODUCTION

Material developments over the past few years have provided the Army with a class of materials generically referred to as high fragmentation steel. This includes not only HF-1 steel heat treated to a variety of conditions, but also a number of other steels such as 1340, 9260, 52100 and PR-2 specifically heat treated to provide good fragmentation characteristics. When heat treated for maximum fragmentation, these materials offer a potential for a severalfold increase in the fragmentation performance of naturally fragmenting artillery projectiles.

These improvements in fragmentation, however, are generally accompanied by a decrease in the flaw tolerance of the materials; so much so, that a substantial degree of caution must be exercised in applying these materials to the manufacture of a high volume production item like a conventional artillery projectile which is subjected to a relatively severe field life. The need for this caution was explicitly cited for the proposed use of isothermally transformed HF-1 steel in the 155 mm, M107E1 projectile in a report[1] by a National Materials Advisory Board Ad Hoc Committee on Shell Steel.

In relation to this, the U. S. Army Armament Command (ARMCOM) has developed a Program on Fragmentation Materials for Artillery Projectiles[2] which is aimed at: (1) evaluation the material safety and reliability of isothermally transformed HF-1 steel in the M107E1 projectile; (2) exploring improved NDT techniques for potential use in screening the relatively small critical flaw sizes expected to be associated with high fragmentation projectiles; (3) determining the relative dynamic fracture resistance of materials represented in the current artillery munitions stockpile; and (4) assessing the relative merits of alternative materials/concepts for achieving improved fragmentation performance in artillery projectiles.

The present report summarizes the results of the first part of that program, that is, an evaluation of the material safety and reliability of isothermally transformed HF-1 steel in the M107E1 projectile. This evaluation is developed in terms of the critical flaw sizes associated with each of the major sources of stress to which the projectile is subjected in the course of deployment and firing. A critical flaw is considered to be one which would cause unstable or catastrophic crack growth to occur in the presence of a given tensile stress.

---

1 "Producibility of Artillery Shells Made from HF-1 Steel", National Materials Advisory Board, Report NMAB-307, April 1973.

2 "Program Plan on Fragmentation Materials for Artillery Projectiles", U.S. Army Armament Command, 15 April 1974.

## APPROACH

If high fragmentation (and inherently brittle) materials are to be used successfully in artillery projectiles, it is essential that their safety and reliability be accurately assessed in terms of flaws which would be critical with respect to loss of material integrity when subjected to the forces associated with rough handling in the field and those encountered in launch. Description of these critical flaws in terms of their sizes, locations and orientations would provide a basis for (1) assessing the stringency of quality control necessary to meet production requirements with an acceptably low rejection rate, and (2) establishing final inspection standards to insure the safety of finished projectiles.

The most accurate and quantitative means of describing critical flaws is through the use of linear elastic fracture mechanics concepts. This methodology has been successfully applied to problems in a number of areas including the design of pressure vessels and the development of rocket motor casings, missile casings, high performance aircraft components and rotor generator forgings.

With respect to gun launched projectiles, fracture mechanics concepts have been applied by the Navy[3] in the development of an improved five inch projectile and by AMMRC in the analysis of permissible flaws for projectiles[4]. More recently, Frankford Arsenal has applied fracture mechanics to problems relating to the integrity of the 155 mm, M121 chemical shell[5] and is currently using a fracture mechanics approach to establish inspection criteria for the 155 mm, M549 RAP warhead.

## PROCEDURE

Analytically, critical flaw size is defined by an expression of the type shown below:

$$a_c = f\left[Q\left(\frac{K_{IC}}{\sigma}\right)^2\right]$$

3 R. W. Lowry, "Evaluation and Selection of Alternate Steels for the Improved 5"/54 Projectile Body", Naval Weapons Laboratory Report, TR-2585, July 1971.

4 F. I. Baratta, "Fracture Mechanics Approach to the Design of Projectiles", AMMRC Report, TN 69-05, July 1969.

5 J. H. Mulherin, "General Support Engineering, 155 mm, M107 HE Projectile", Frankford Report, R-2047, July 1972.

where:

$a_c$ = critical flaw depth

Q = a parameter which takes into account the shape and notch acuity of the flaw

$K_{IC}$ = plane strain fracture toughness of the material

$\sigma$ = the tensile component of stress acting normal to the plane of the flaw

The procedure involved in defining critical flaw sizes in the M107E1 projectile, therefore, consisted of: (1) determining the dynamic fracture toughness of the projectile material; (2) determining the distribution and magnitude of the tensile components of stress to which the projectile would be subjected in its life cycle; (3) identifying the depth and orientation of flaws which, on the basis of the fracture toughness and stress factors, could result in rapid crack propagation; and (4) testing intentionally pre-flawed projectiles to confirm the calculated critical flaw size values. The major factors considered in each of these steps are discussed in the following paragraphs.

## Fracture Toughness

Since plane strain fracture toughness is a structure sensitive material characteristic similar to tensile and impact properties, it is dependent upon material condition, strain rate and temperature. In assessing the safety of using isothermally transformed HF-1 steel in the M107 projectile its fracture toughness was, therefore, determined under a sufficiently wide variety of conditions to allow realistic assessment of the minimum value likely to be encountered in a fielded projectile.

The various conditions included:

(1) material representing three commercial heats of HF-1

(2) material from both rolled plate and forged projectiles

(3) Strain rates (as determined from load rise times) ranging from quasi-static ($\sim 10^{-4}$ in/in/sec) to rates comparable to those encountered by a projectile in launch or drop ($\sim$25 in/in/sec)

(4) Test temperatures of -65, +70 and +200 degrees F

Metallurgical characterization of the material was also made with respect to chemical composition, microstructure, impact toughness and tensile properties. In addition, a limited amount of low cycle fatigue information was also generated to determine the likelihood of sub-critical crack growth occurring during repeated loads encountered in the multiple drop sequence which TECOM uses to simulate rough handling.

## Stress Analysis

In order to develop the necessary information on the distribution and magnitude of stresses and the rates of loading experienced by the M107E1 projectile, both analytical and experimental studies of launch and rough handling conditions were performed at the Feltman Research Laboratory, Picatinny Arsenal.

Finite element methods of stress analysis which address the effects of band engraving pressure, inertial and rotational forces, and the contributions of the explosive filler to the distribution of loads within the projectile were available for launch conditions. However, additional refinements were made with respect to the interaction between the filler and the projectile metal part. Instrumented firings were then performed to compare the refined analysis with the actual strain experienced by the projectile.

Since balloting is also considered to be an important factor in artillery projectiles, an analysis of the balloting behavior of the M107 was also performed with emphasis directed to the permissible individual maximum pressure condition.

With respect to rough handling, field conditions are not well defined and the general magnitude of the forces encountered is not known. To address this area, TECOM drop test requirements were used as the basis for evaluating rough handling. Specific stress and loading rate data were developed through a series of drop tests of instrumented projectiles.

Although the Picatinny analysis addressed both effective stresses and the distribution of tensile components of stress, only the latter enter into critical flaw size determinations. Picatinny Arsenal's effort will not be discussed in detail in this report, but rather, will be summarized in terms of the general factors considered and the resulting tensile stresses of significance.

## Critical Crack Sizes

With respect to the safety and reliability of a projectile, the primary concern is the possibility of fracture occurring at stresses below the tensile-yield strength of the projectile material. In the case of materials of relatively low toughness, sub-yield strength

fracture can result from the presence of defects of a critical size or larger. In the presence of a defect, the potential for catastrophic failure depends upon the size and shape of the defect, the fracture toughness of the material, and the magnitude of the opening mode or tensile stress acting across the defect.

The relationship between these factors is given by:

$$a_c = \frac{1}{\pi} \arctan \left[ \frac{Q}{(1.1)\ 2} \left( \frac{K_{IC}}{\sigma} \right)^2 \right]$$

where:

$a_c$ = critical crack size (depth)

$Q$ = a flaw shape parameter

$K_{IC}$ = plane strain fracture toughness

$\sigma$ = tensile component of stress acting normal to the plane of the crack

A general expression for Q is:

$$Q = E_k^2 - 0.212 \left( \frac{\sigma}{\sigma_{ys}} \right)^2$$

in which $E_k$ is a complete elliptic integral of the second kind.

$$E_k = \int_0^{\frac{\pi}{2}} \left[ 1 - \frac{c^2 - a^2}{c^2} \sin^2 \theta \right]^{\frac{1}{2}} d\theta$$

In the present work, the most severe type of defect (an infinitely long sharp crack) was closely approximated by assuming a semi-elliptical crack with a ratio of semi-minor axis (a) to major axis (2c) equal to 0.1. Q was then evaluated using the Tiffany-Lorentz Chart shown in Figure 1.

Also, to address the most severe case, the lower shelf value of fracture toughness observed in the material characterization study and the highest tensile stresses indicated by the stress analysis were used in calculating the critical crack sizes.

From the relationships shown above, it is possible to develop a mapping of critical flaw sizes throughout the entire projectile. For the present purposes, however, the size, location and orientation of only the smallest critical flaw for each of the major sources of stress (inertial, engraving and balloting forces in launch and impact forces in rough handling) have been identified.

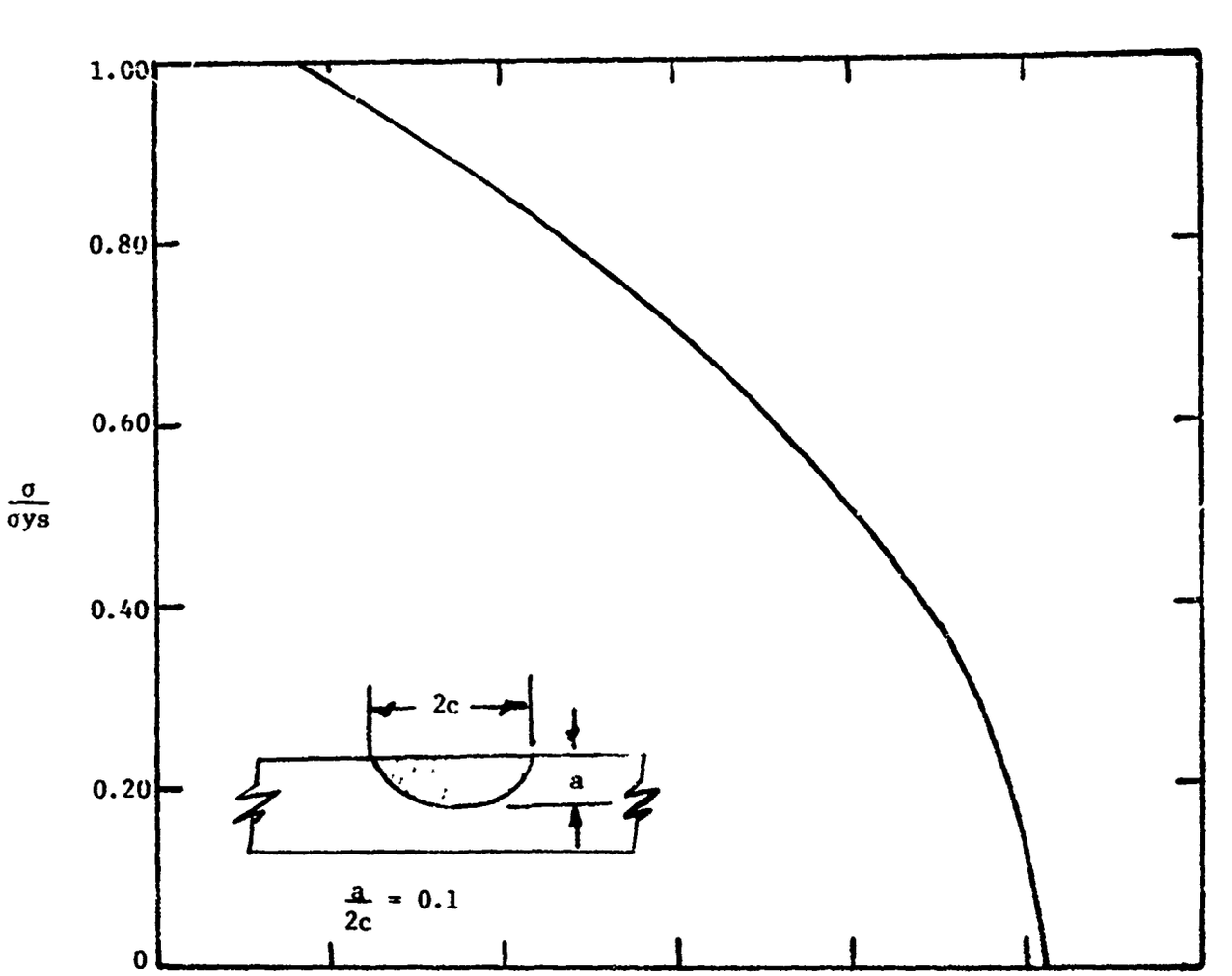


**Figure 1.** Tiffany-Lorentz chart of the flaw shape parameter for elliptical cracks.

## Drop Testing of Pre-flawed Projectiles

In order to confirm the calculated critical crack sizes, a number of intentionally preflawed M107E1 projectiles were subjected to drop tests.

Flawing was accomplished by machining narrow elliptical notches ($\frac{a}{2c} \leq 0.1$) of selected depths into the projectile wall using an electric discharge (EDM) process. For the most part, these notches were on the order of 0.005" wide and, where possible, were sharpened by subjecting the projectiles to cyclic hydrostatic pressurization to initiate a small fatigue crack at the root of the notch. Notch depths were selected to range from well below to well above the calculated critical sizes.

# RESULTS

## Fracture Toughness and Material Characterization

### Chemical Composition

Studies were performed on isothermally transformed HF-1 steel representing two heats of material in the form of plate and a third heat in the form of M107E1 projectiles.

Chemistries of the three heats of HF-1 are given in Table 1 along with HF-1 specification ranges. It can be seen that the compositions of all three materials essentially satisfy specification requirements. Moreover, all three heats are nearly identical in composition. Even the difference in silicon content between the projectiles and the two plate samples can be considered minor.

### Structure

Heat treatment of the plate material was performed on rough machined test specimens and involved austenizing at 1700 degrees F followed by a quench to 1150 degrees F, holding at 1150 degrees F for 1½ hours, and then air cooling to room temperature. The projectiles were heat treated in production using a 1650 degrees F austenitizing temperature and isothermal transformation for 1½ hours at 1150 degrees F.

Representative microstructures for the three materials are shown in Figures 2 - 4, inclusive. As expected, the microstructures developed by the isothermal transformations represent essentially a pearlite matrix with some evidence of the beginnings of a partial carbide network.

An examination of the macroetched sections of the M107E1 projectiles showed flow line patterns of the type normally associated with hot forged shell bodies. A macrophotograph of the base area is shown in

Table 1. Chemical Compostion (Weight Percent) of HF-1 Steel

| Element | Specification | Heat A | Heat B | Projectile |
|---|---|---|---|---|
| Carbon | 1.00/1.15 | 1.07 | 1.06/1.07 | 1.08 |
| Manganese | 1.70/2.10 | 1.85 | 1.80 | 1.75 |
| Phosphorous | 0.040 Max | .001 | .010 | .001 |
| Sulfur | 0.035 Max | .013 | .013 | .020 |
| Silicon | 0.70/1.00 | 1.02 | 1.03 | .89 |
| Nickel | 0.25 Max | 0.04 | 0.04 | .02 |
| Chromium | 0.20 Max | .05 | 0.07 | .03 |
| Molybdenum | 0.06 Max | < .01 | < .01 | < .01 |
| Copper | 0.35 Max | < .05 | < .05 | < .05 |
| Vanadium | --- | < .01 | < .01 | < .01 |
| Aluminum | 0.020 Max | < .01 | < .01 | < .01 |

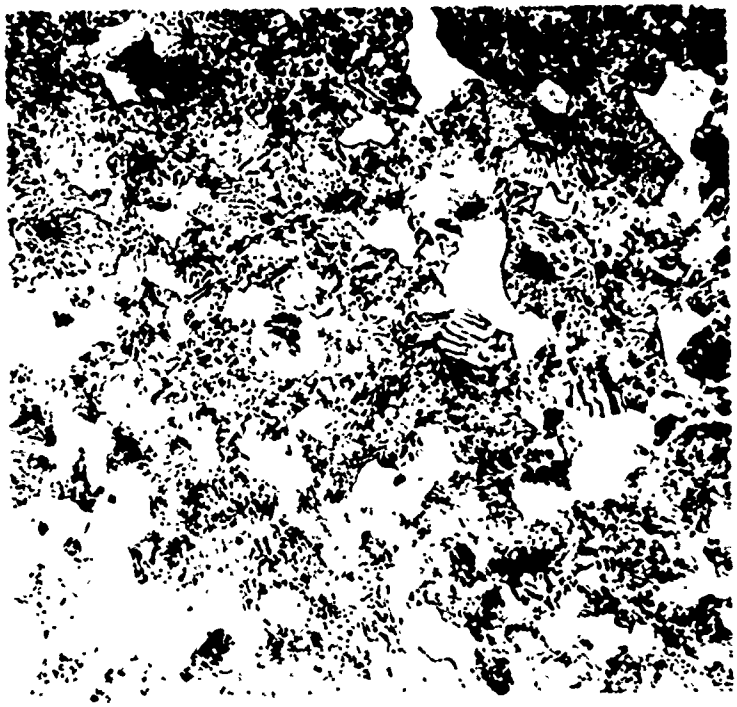

Nital 500X

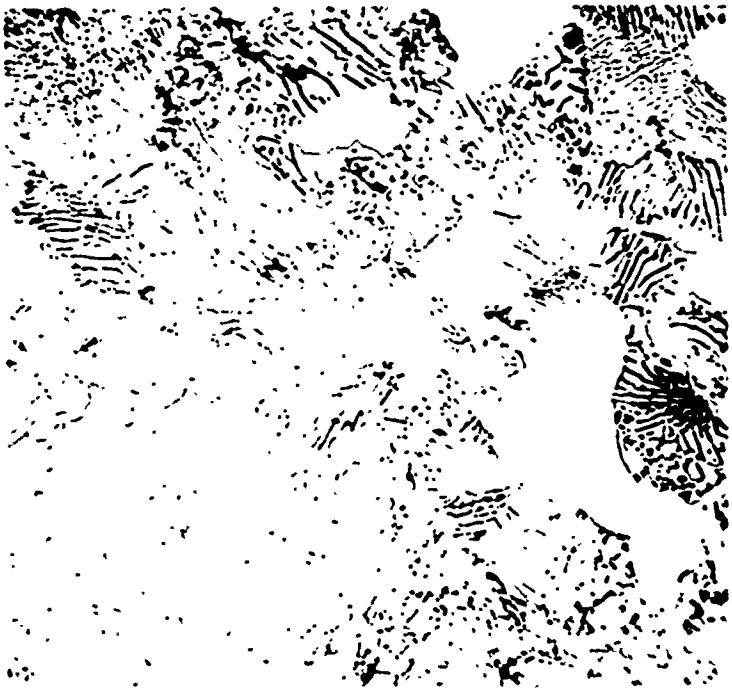

Nital 1000X

Figure 2. Photomicrographs of Heat A, isothermally transformed HF-1.

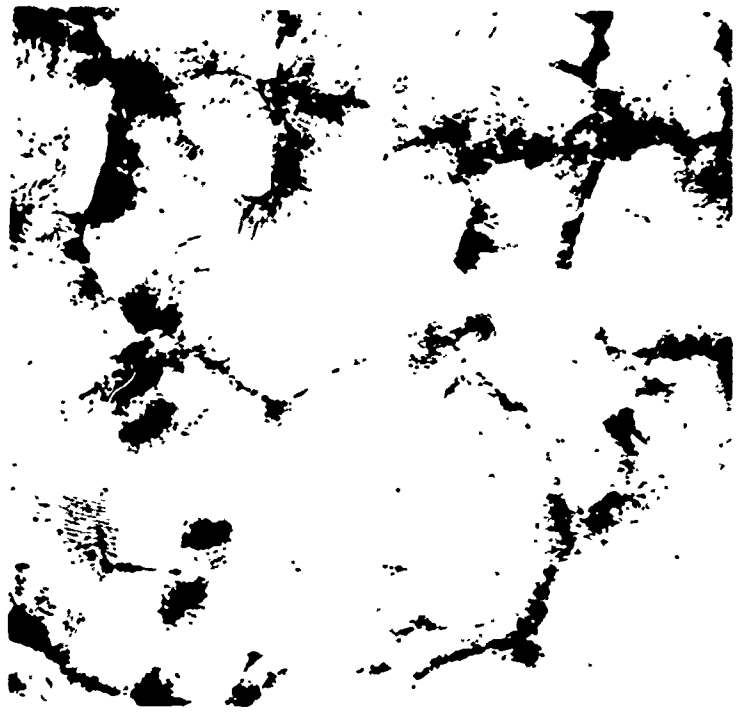

Nital 500X

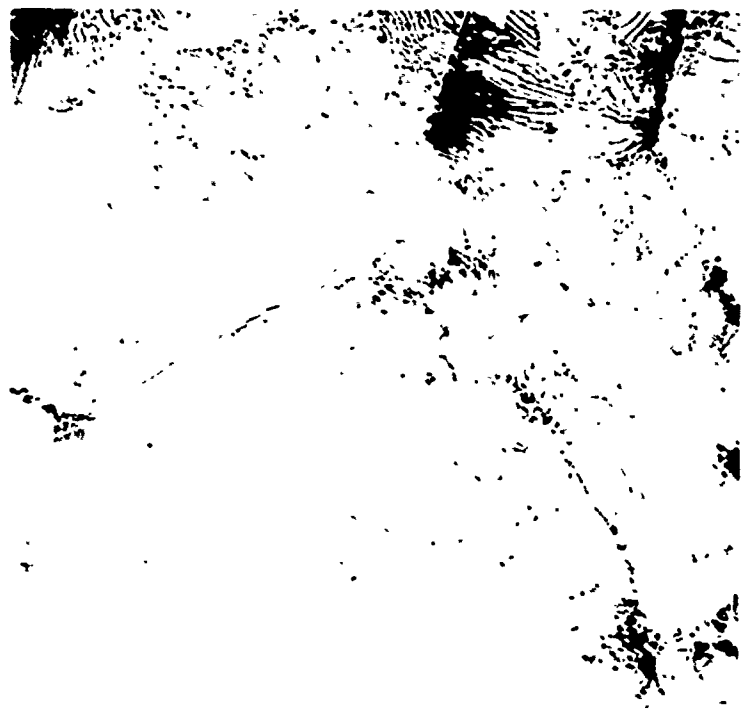

Nital 1000X

**Figure 3. Photomicrographs of Heat B, isothermally transformed HF-1.**

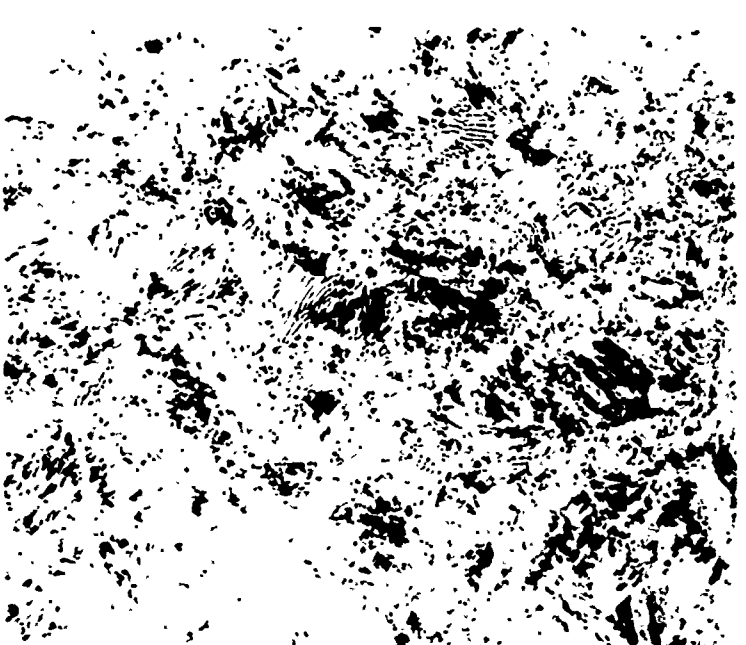

Nose 500X

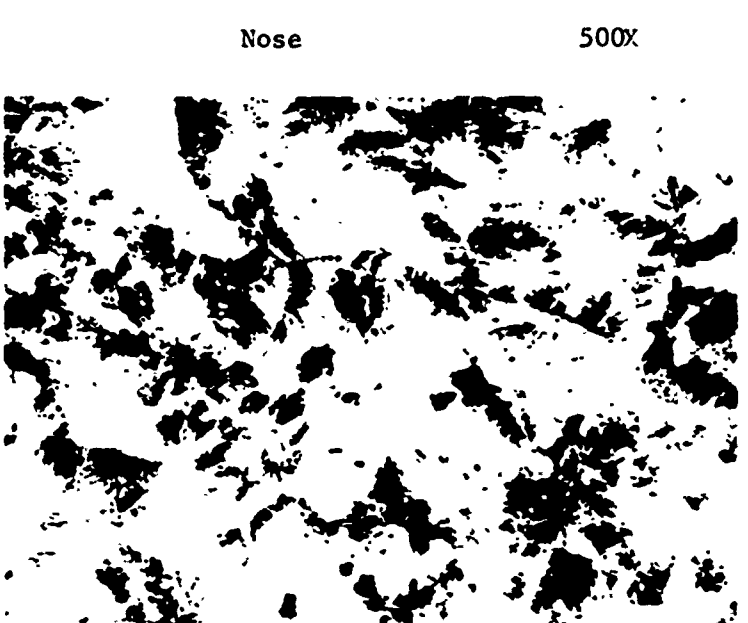

Lower Sidewall 500X

Figure 4. Photomicrographs of the nose and lower sidewall regions of M107E1 projectiles, isothermally transformed HF-1.

Figure 5. Of particular interest is the area in the center of the base where irregular metal flow has occurred. This area could be expected to be more susceptible to the formation of both subsurface and surface cracks than other regions of the projectile.

## Engineering Mechanical Properties

Results of engineering mechanical property determinations of Heat A are presented in Table 2. The data was obtained using 0.252 in. diameter tensile specimens with a gage length of 1.4 in. Examination of the date indicates both temperature and strain rate sensitivities insofar as strength is concerned. Both ultimate tensile strength and tensile yield strength increase with decreasing temperature and with increasing strain rate. The ductility properties, on the other hand, show a definite trend toward higher values with increasing temperature, but no consistent trend with respect to strain rate. The tensile and yield strength data are shown graphically in Figures 6 and 7, respectively.

Results of the tensile property determinations on Heat B, which were performed by the Mechanics Division of AMMRC, are shown in Figures 8 and 9. These properties show a material behavior pattern similar to that of Heat A, but with strength levels approximately 15 KSI lower.

Room temperature, quasi-static properties of longitudinal specimens taken from the lower sidewall of two M107E1 projectiles are given in Table 3. While the yield strength of the projectile material is of the same order of magnitude as that of Heat A, its ultimate tensile strength is noticeably lower than that of either Heat A or Heat B. Also, both the elongation and reduction in area of the specimens from projectiles are approximately double those obtained from Heat A.

## Impact Toughness

The impact toughness of Heat A was investigated at test temperatures ranging from -65 degrees F to +1150 degrees F using Charpy V-notch specimens. The data obtained are listed in Table 4 and shown graphically in Figure 10. Impact toughness values for this material ranged from 2.44 ft-lbs at -65 degrees F to 8.33 ft-lbs at 1150 degrees F. Since no distinct toughness transition was observed, the toughness can be considered as still representing lower shelf values even at the highest test temperature investigated.

## Fracture Toughness

Fracture toughness determinations were made on all three materials over the same ranges of temperature and strain rate for which tensile properties had been obtained.

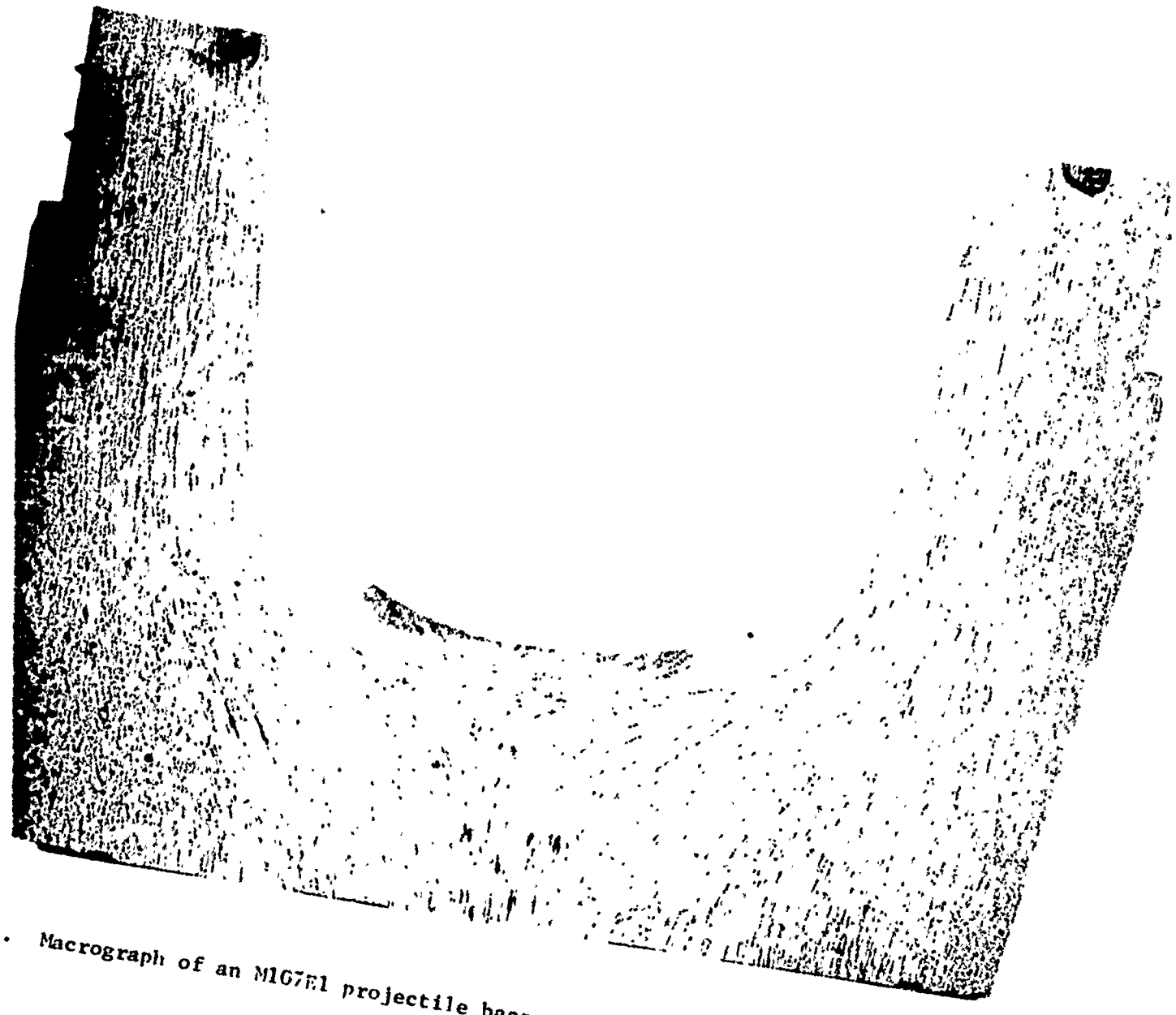

Figure 5. Macrograph of an M107E1 projectile base region, isothermally transformed HF-1.

Table 2. Engineering Mechanical Properties of HF-1 Steel (Heat A) in the Isothermally Transformed Condition

| Testing Temperature (°F) | Strain Rate ($sec^{-1}$) | $\sigma_{ys}$ (0.2%) (ksi) | $\sigma_{ut}$ (ksi) | Elong (1.4 in) (%) | R. A. (%) |
|---|---|---|---|---|---|
| -65 | $10^{-4}$ | 91.4 | 168.7 | -- | -- |
| " | " | 97.6 | 180.8 | 7.4 | 9.3 |
| " | 1.6 | 116.7 | -- | 3.6* | 4.5 |
| " | 1.7 | 122.5 | 191.4 | -- | -- |
| " | 7.2 | 132.1 | 194.7 | -- | -- |
| " | 10.1 | 132.1 | 192.7 | 5.1 | 5.0 |
| " | 19.6 | 126.0 | 194.8 | 4.9 | 7.7 |
| 72 | $10^{-4}$ | 89.4 | 168.7 | 7.3 | 13.1 |
| " | $10^{-4}$ | 85.4 | 161.6 | 8.1 | 12.6 |
| " | 0.75 | 103.7 | 176.6 | 7.7 | 14.6 |
| " | 8.9 | 96.5 | 171.1 | 7.9 | 14.1 |
| " | 17.1 | 97.0 | 176.9 | 8.7 | 12.9 |
| " | 25.3 | 101.6 | 181.0 | 9.0 | 13.6 |
| 200 | $10^{-4}$ | 82.2 | 157.2 | 8.1 | 14.7 |
| " | 1.7 | 95.0 | 162.6 | 7.4 | 15.2 |
| " | 6.4 | 82.9 | 167.5 | 8.1 | 12.5 |
| " | 16.1 | 91.9 | 172.0 | -- | -- |
| " | 20.8 | 91.5 | 169.5 | 8.3 | 15.7 |

* Broke at gage marks

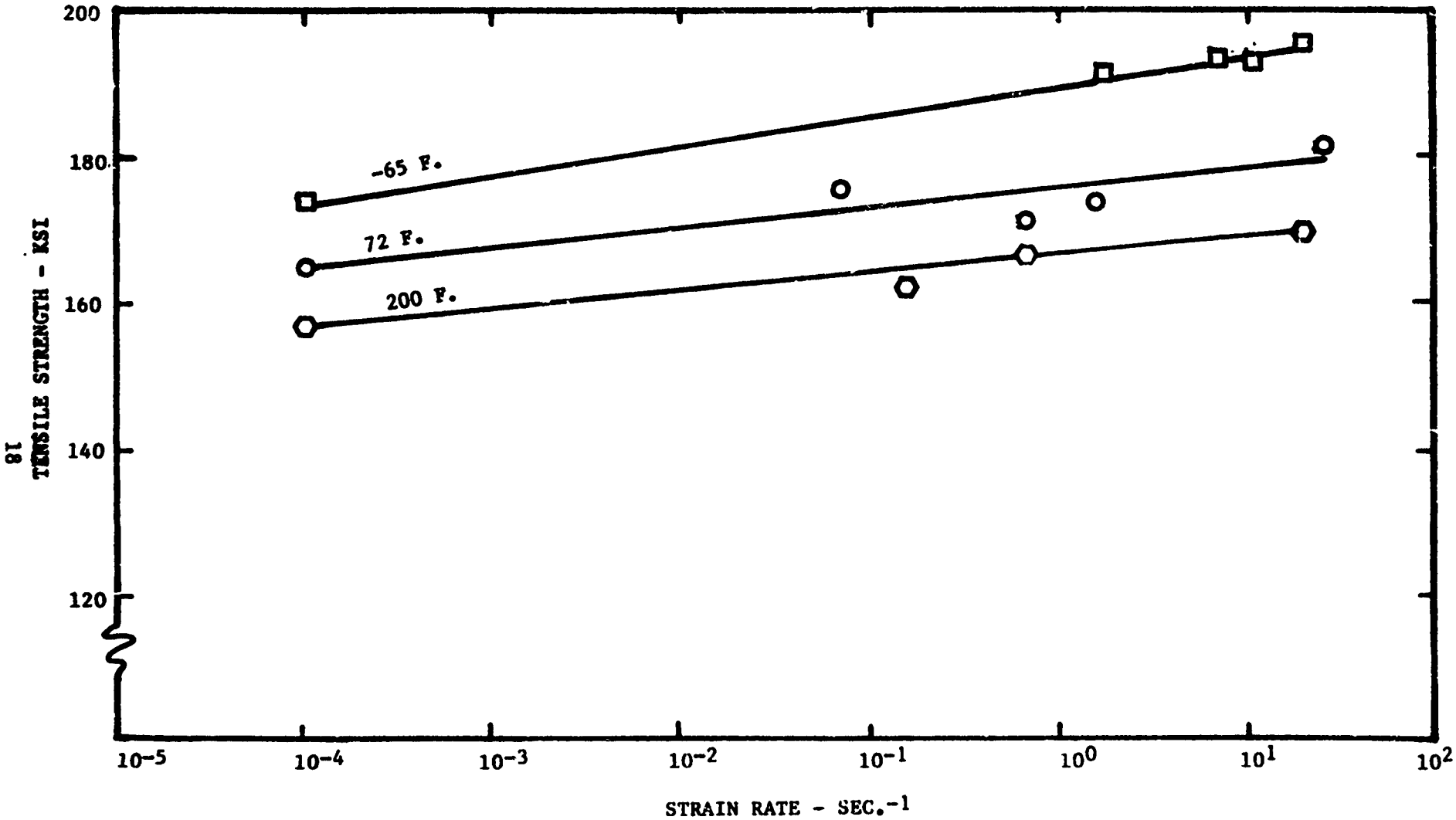


Figure 6. Tensile strength of Heat A, isothermally transformed HF-1, as a function of strain rate and temperature.

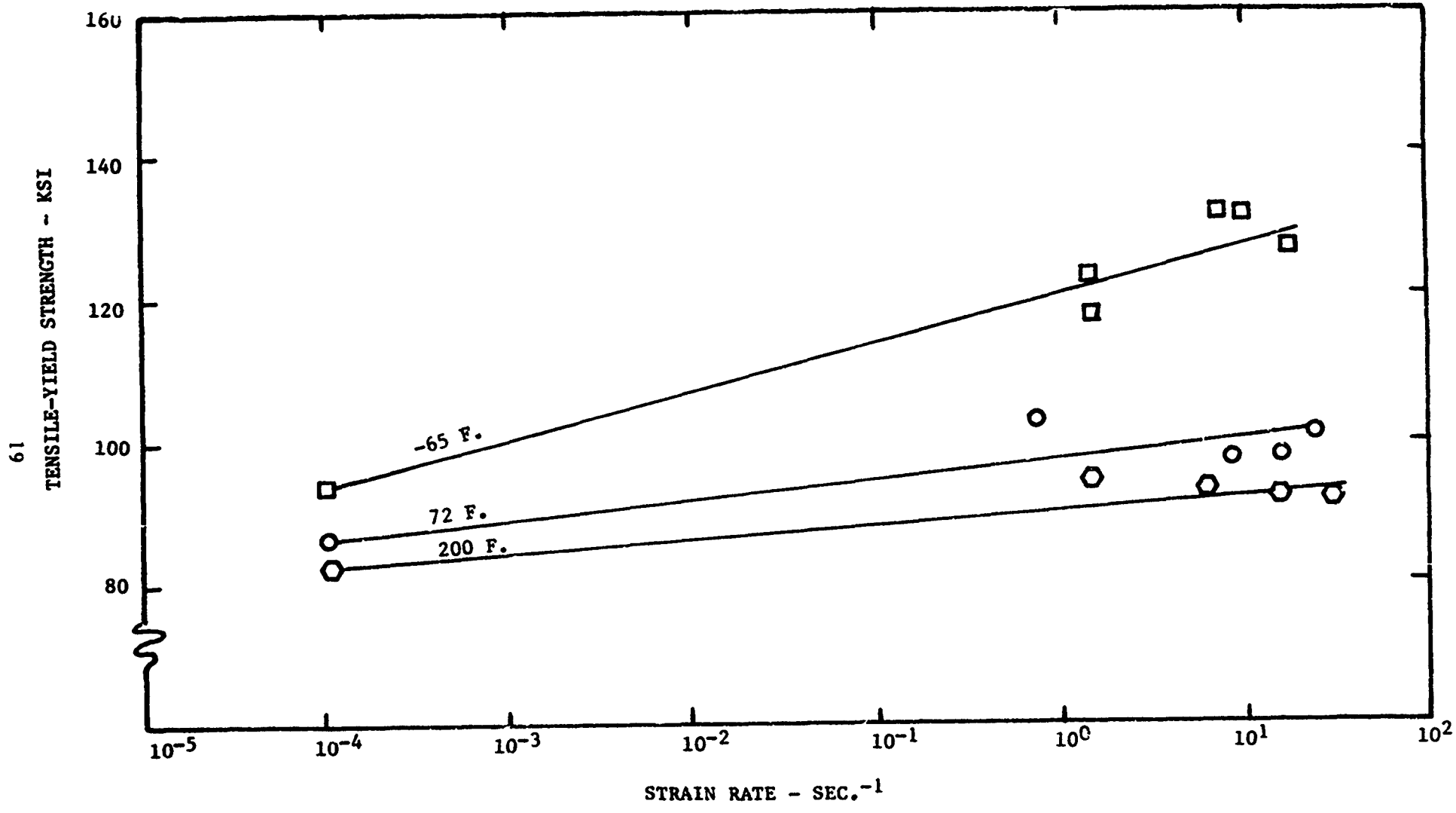


Figure 7. Tensile-yield strength of Heat A, isothermally transformed IT-1, as a function of strain rate and temperature.

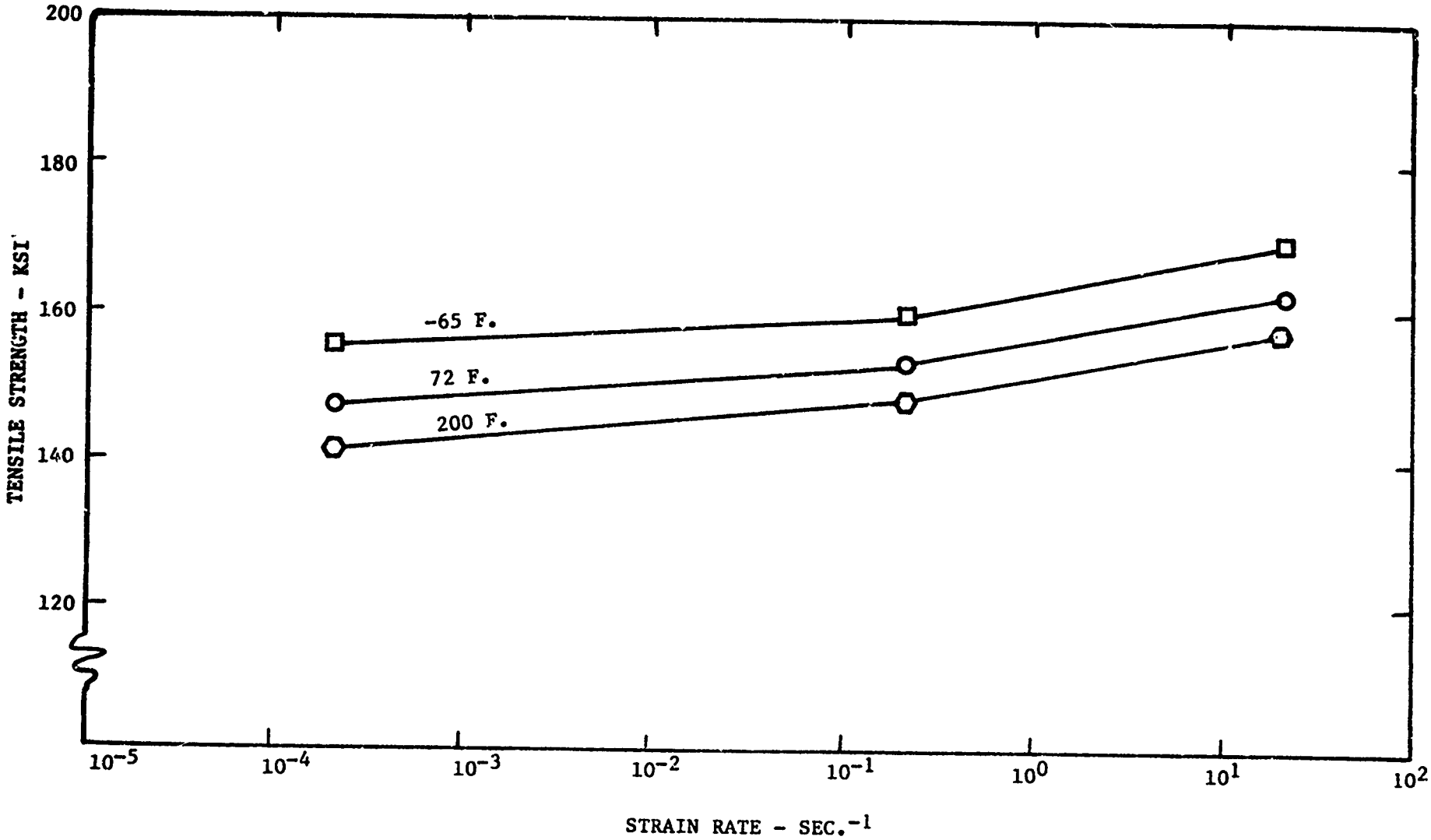


Figure 8. Tensile strength of Heat B, isothermally transformed HF-1 as a function of strain rate and temperature.

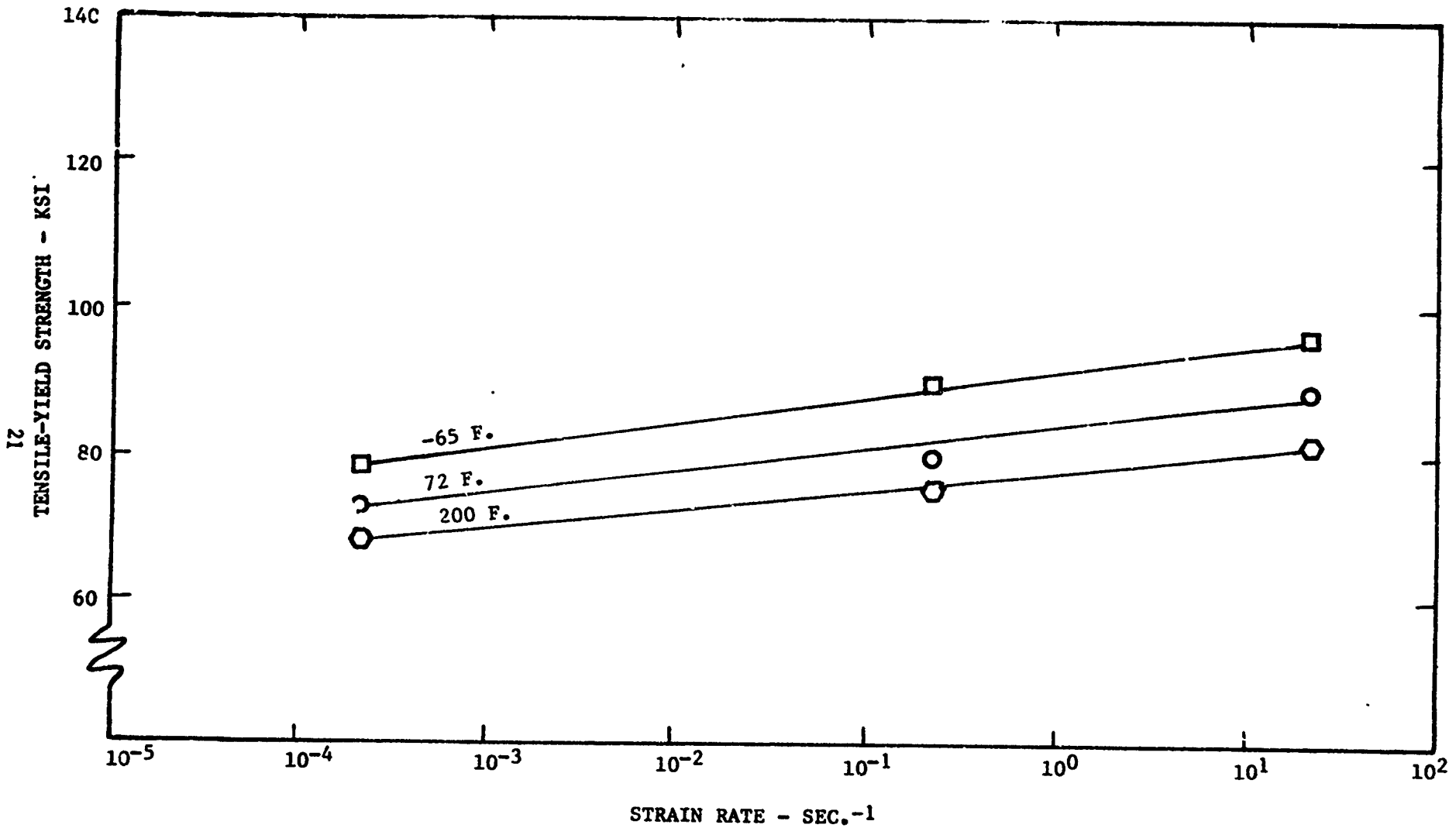


Figure 9. Tensile-yield strength of Heat B, isothermally transformed HF-1, as a function of strain rate and temperature.

Table 3. Engineering Mechanical Properties of M107E1 Projectiles

| Yield Strength 0.1% Offset (psi) | Tensile Strength (psi) | Elongation in 0.640 In. Gage Length (psi) | Reduction of Area (%) |
|---|---|---|---|
| | Projectile No. 1 | | |
| 71,400 | 124,900 | 15 | 37 |
| 69,900 | 123,500 | 16 | 36 |
| 70,100 | 124,500 | 15 | 36 |
| 71,600 | 127,400 | 15 | 34 |
| | Projectile No. 2 | | |
| 61,400 | 131,300 | 11 | 24 |
| 67,400 | 133,300 | 11 | 24 |
| 65,900 | 132,800 | 10 | 22 |
| 67,400 | 131,300 | 12 | 22 |

Table 4. Charpy V-Notch Impact Energy of Isothermally Transformed HF-1 Steel (Heat A) as a Function of Testing Temperature

| Testing Temperature ($^{o}$F) | Impact Energy (ft/lbs.) | | | Average Impact Energy (ft/lbs) |
|---|---|---|---|---|
| -65 | 2.48 | 2.25 | 2.60 | 2.44 |
| 68 | 3.95 | 3.40 | 3.51 | 3.62 |
| 150 | 3.80 | 3.05 | 2.90 | 3.25 |
| 400 | 3.95 | 4.20 | 3.65 | 3.93 |
| 600 | 5.00 | 5.00 | 5.10 | 5.03 |
| 800 | 6.20 | 6.60 | 7.70 | 6.83 |
| 1150 | 8.00 | 7.40 | 9.60 | 8.33 |

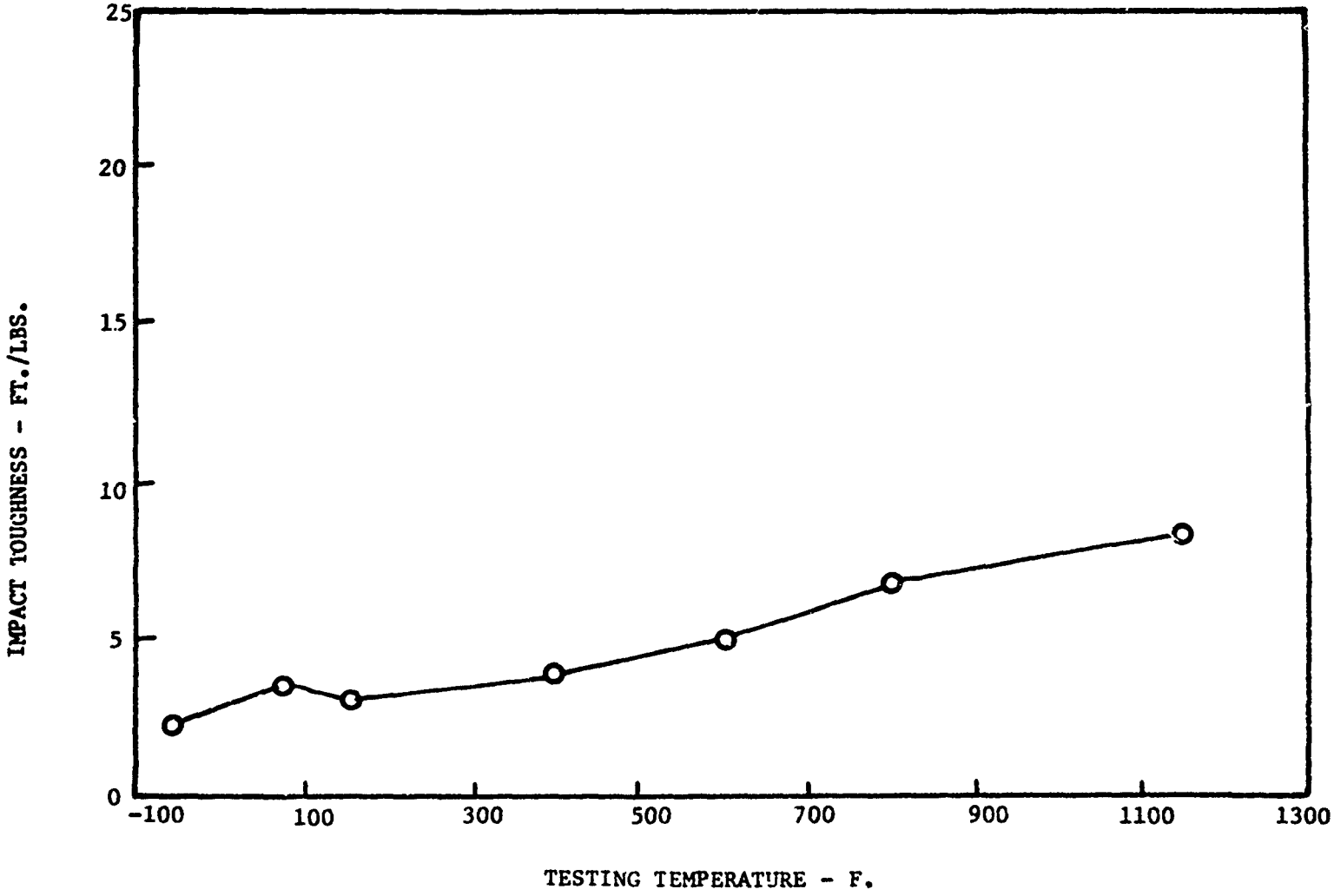


Figure 10. Charpy V-Notch impact toughness of Heat A, isothermally transformed HF-1.

Tests on the two heats of plate material were made using 1 in. thick compact tension (CKS) specimens and the testing procedures conformed to the recommendations of ASTM committee E-24, with one exception. This involved the use of a strain gage transducer on the back side of the specimen, rather than the usual double cantilever clip gage, to detect crack opening displacement as a function of load in the high strain rate tests.

Loading was controlled by means of a quartz crystal load transducer and a ramp function signal. Load-strain and time mark traces were recorded photographically from a dual beam oscilloscope. In general, the materials exhibited linear load-strain response up to the point of crack instability. Conventional methodology was used to calculate the fracture toughness.

Strain rates were calculated from the rise time to crack instability using the following relationship:

$$\dot{\varepsilon} = \frac{2\sqrt{3}\ \sigma_{ys}}{ET}$$

where:

$\dot{\varepsilon}$ = strain rate in in/in/sec

$\sigma_{ys}$ = tensile yield strength (for the temperature and strain rate involved) in psi

E = Young's Modulus in psi

T = rise time to crack instability in sec.

and:

The factor $2\sqrt{3}$ is the plane strain plastic constraint factor for the crack.

Fracture toughness results from Heat A are shown in Table 5 and Figure 11. Examination of the data reveals two significant findings. First of all, the fracture toughness of isothermally transformed HF-1 steel is noticeably sensitive to test temperature. Fracture toughness decreases significantly with decreasing test temperature at all strain rates. Secondly, at any given temperature, fracture toughness appears to decrease slightly in going from quasi-static to intermediate strain rates and then rise again at higher strain rates. This rise with increasing strain rates is more pronounced at the higher testing temperatures.

Fracture toughness results from Heat B are shown in Table 6 and Figure 12. Although more limited in scope, these results are in substantial agreement with those of Heat A.

Table 5. Plane Strain Fracture Toughness of HF-1 Steel (Heat A) in the Isothermally Transformed Condition

| Testing Temperature ($^{o}$F) | Strain Rate ($sec^{-1}$) | B (in.) | a (in.) | P (lbs) | $K_{IC}$ (ksi $\sqrt{in.}$) |
|---|---|---|---|---|---|
| -65 | $10^{-4}$ | 1.00 | 1.162 | 2400 | 21.4 |
| " | " | " | 1.149 | 2290 | 19.9 |
| " | 4.4 | " | 1.017 | 2600 | 18.1 |
| " | 22.9 | " | 1.155 | 2700 | 23.8 |
| " | 29.8 | " | 1.141 | 2750 | 23.6 |
| " | 29.8 | " | 1.017 | 3200 | 22.3 |
| " | 29.8 | " | 1.034 | 2700 | 19.3 |
| " | 29.8 | " | 1.033 | 2700 | 19.3 |
| " | 59.6 | " | 1.165 | 2100 | 18.8 |
| " | 59.6 | " | 1.152 | 2250 | 19.7 |
| 72 | $10^{-4}$ | " | 1.193 | 2630 | 24.8 |
| " | 1.1 | " | 1.165 | 2600 | 23.3 |
| " | 15.2 | " | 1.146 | 2900 | 25.0 |
| " | 22.7 | " | 1.161 | 2850 | 25.2 |
| " | 37.9 | " | 1.171 | 3310 | 30.0 |
| " | 45.5 | " | 1.164 | 3200 | 28.5 |
| 200 | $10^{-4}$ | " | 1.185 | 3330 | 31.0 |
| " | $10^{-4}$ | " | 1.139 | 3490 | 29.8 |
| " | 16.4 | " | 1.152 | 3300 | 28.8 |
| " | 21.3 | " | 1.156 | 3600 | 31.7 |
| " | 42.5 | " | 1.142 | 4200 | 36.0 |
| " | 42.5 | " | 1.158 | 4200 | 37.0 |

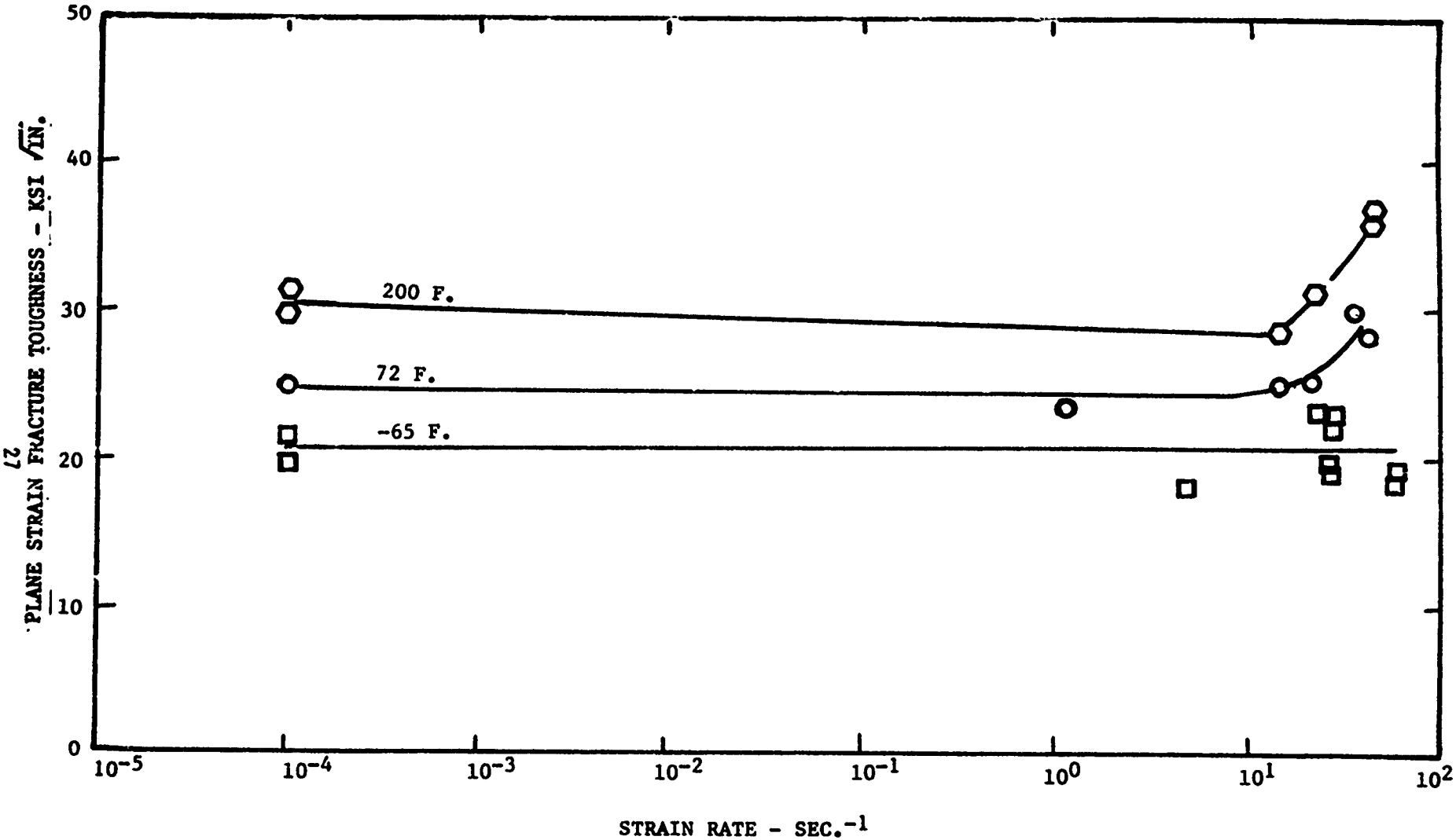


Figure 11. Plane strain fracture toughness of Heat A, isothermally transformed HF-1, as a function of strain rate and temperature.

Table 6. Plane Strain Fracture Toughness of HF-1 Steel (Heat B) in the Isothermally Transformed Condition

| Testing Temperature (°F) | Strain Rate ($sec^{-1}$) | $K_{IC}$ (ksi $\sqrt{in}$) |
|---|---|---|
| 225 | $2X10^{-4}$ | 36.33 |
| " | " | 38.40 |
| " | " | 38.72 |
| " | $10^{1}$ | 40.09 |
| " | " | 34.21 |
| " | " | 39.35 |
| " | " | 34.56 |
| 80 | $2X10^{-4}$ | 24.43 |
| " | " | 27.08 |
| " | " | 27.44 |
| " | $2.5X10^{-1}$ | 26.15 |
| " | " | 27.72 |
| " | $10^{1}$ | 29.56 |
| " | " | 29.50 |
| -65 | $2X10^{-4}$ | 19.46 |
| " | " | 19.46 |
| " | $10^{1}$ | 23.44 |
| " | " | 27.95 |
| " | " | 23.74 |

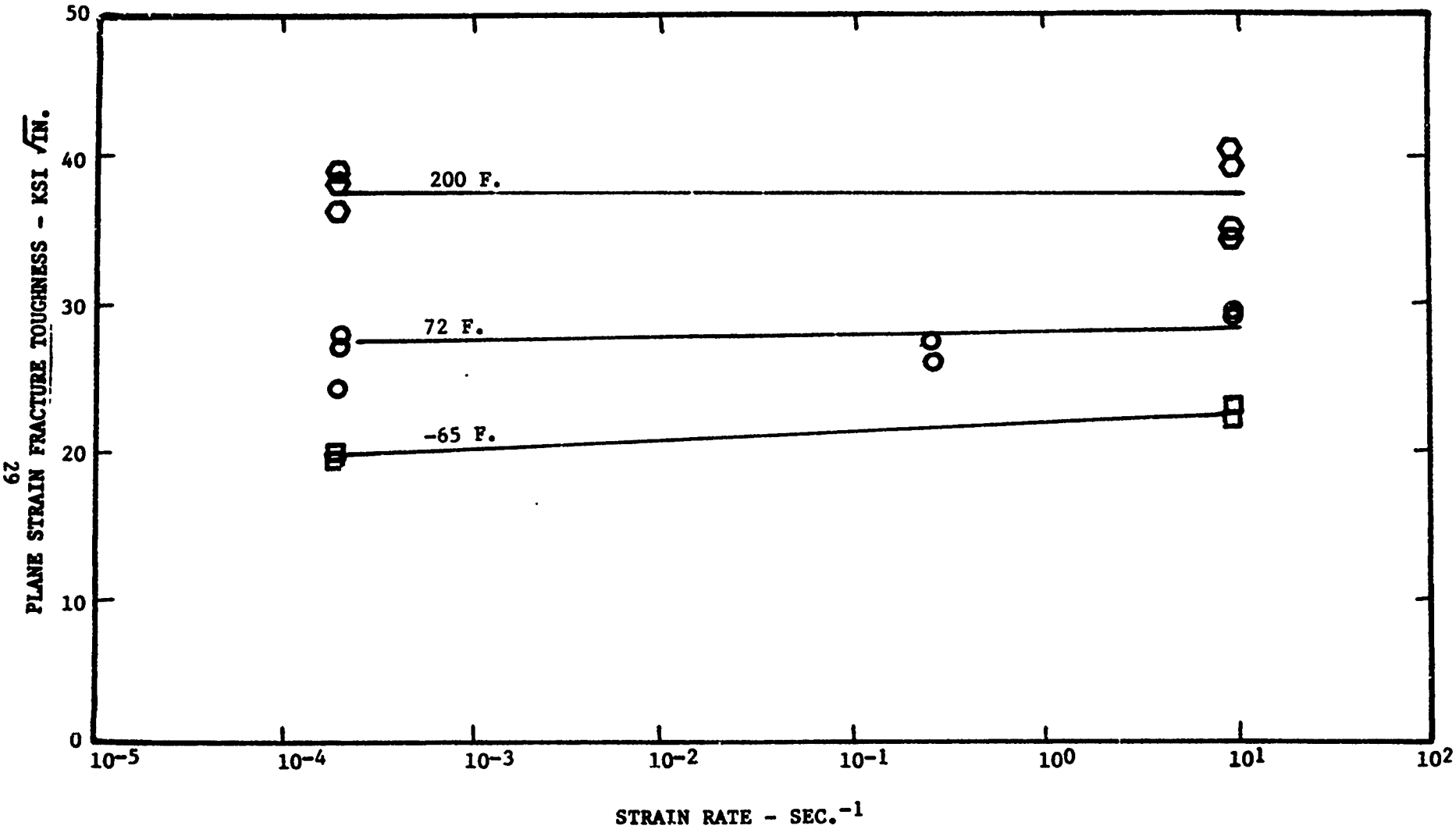


Figure 12. Plane strain fracture toughness of Heat B, isothermally transformed HF-1, as a function of strain rate and temperature.

Fracture toughness determinations were also made on specimens machined directly from M107E1 projectiles. Projectile geometry precluded the use of standard CKS specimens. Instead, properly proportioned longitudinal specimens of a sub-sized bend bar configuration were machined such that the notched sections of the specimens represented material from the region beneath the band seat. The specimens were notched and precracked so that crack propagation was in the through-the-thickness direction. The tests were conducted at a quasi-static strain rate and at ambient laboratory temperature.

Because sub-sized specimens were used, it was necessary to apply a plasticity correction to the results. The plasticity correction used after Irwin[6] was:

$$Kc^2 = K_{IC}^2 \ (1 + 1.4 \ \beta_{IC}^2)$$

where:

$$\beta_{IC} = \frac{1}{B} \left[\frac{K_{IC}}{\sigma_{ys}}\right]^2$$

B = specimen breadth

$K_c$ = elevated mixed mode fracture toughness obtained in the test

The corrected results should be within ±10% of valid $K_{IC}$ values. Comparison of these results, Table 7, with the quasi-static room temperature data obtained from plate material show reasonable agreement with Heat B, but noticeably higher values than Heat A.

Crack Growth Under Repeated Loading

In order to address the question of possible crack growth during repeated loading (e.g. multiple drops in rough handling), room temperature crack growth rate data was obtained on Heat A. This is shown in Figure 13. The broken horizontal line on this diagram represents the minimum room temperature value of $K_{IC}$ observed. As can be seen, the crack growth rate at stress intensities just below this is on the order of $2 \times 10^{-5}$ in./cycle. This would indicate that even at stress intensities approaching $K_{IC}$, the crack growth induced by as many as five repeated loads would still be less than 0.0001 in. and could thus be considered insignificant.

6 G. Irwin, et. al., "Basic Aspects of Crack Growth and Fracture", Naval Research Laboratory Report 6598, November 1967.

Table 7. Fracture Toughness Data for a Circumferentially Oriented Crack in the Through-the-Thickness Direction on the M107E1 Projectile Under the Band Seat

| Specimen Identification | B (In.) | a (In.) | $P_Q$ (Lbs) | $K_Q$ (psi $\sqrt{in.}$) | $2\frac{1}{2}\left[\frac{K_Q}{\sigma_{ys}}\right]^2$ | Corrected $K_{IC}$ (psi $\sqrt{in}$) |
|---|---|---|---|---|---|---|
| 1 - B | 0.250 | 0.279 | 248 | 37,100 | 0.54 | 29,000 |
| 1 - C | 0.250 | 0.275 | 256 | 37,300 | 0.54 | 29,000 |
| 1 - D | 0.250 | 0.279 | 255 | 38,200 | 0.57 | 29,400 |
| 2 - A | 0.250 | 0.261 | 332 | 44,100 | 0.76 | 31,600 |
| 2 - B | 0.250 | 0.263 | 320 | 43,100 | 0.73 | 31,400 |
| 2 - C | 0.250 | 0.275 | 294 | 42,900 | 0.72 | 31,300 |

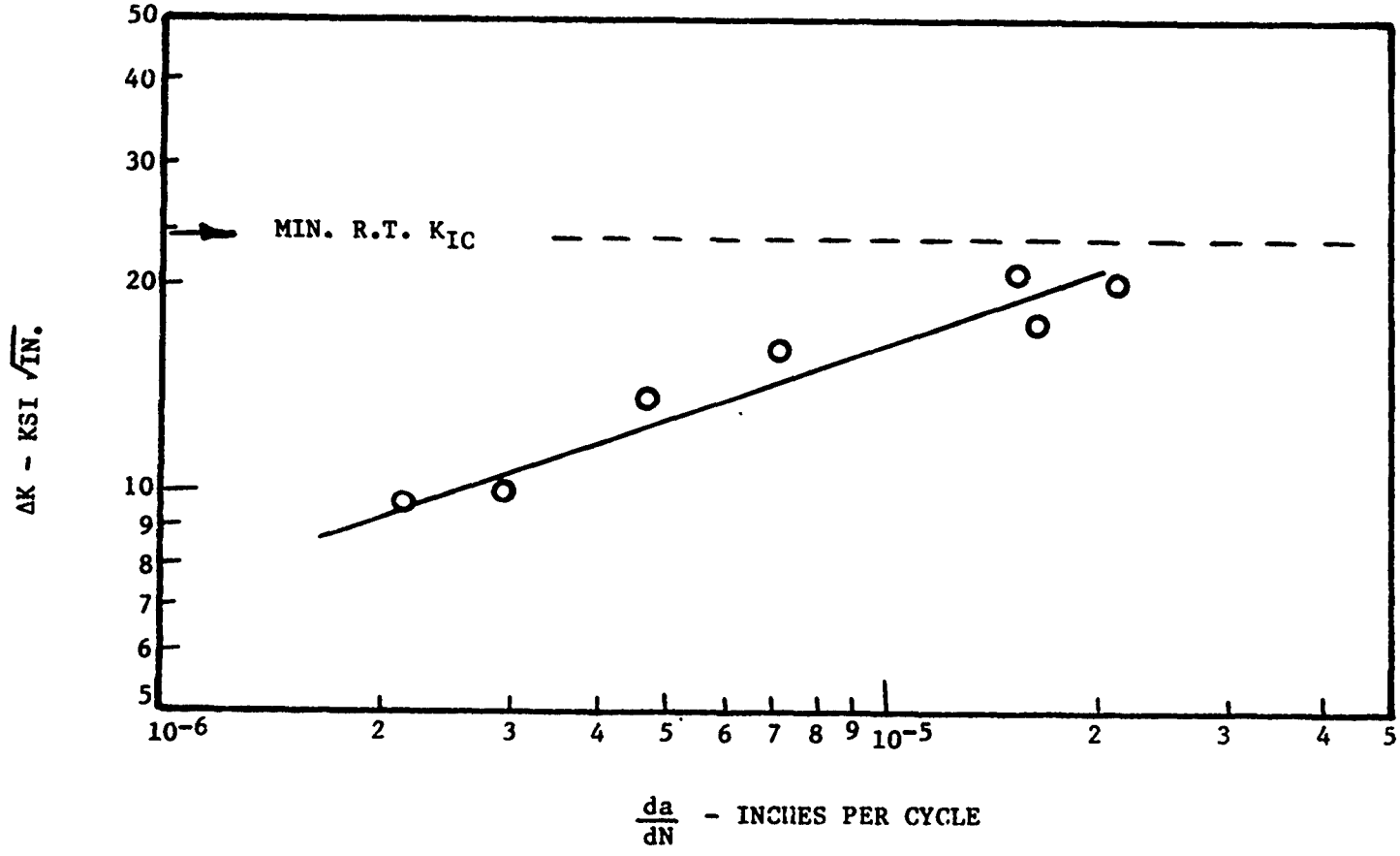


Figure 13. Room temperature crack growth characteristics of HF-1 in the isothermally transformed condition.

## Stress Determinations

### Launch Stresses

Stresses resulting from setback and engraving forces were analytically determined using an elastic-plastic finite element computer program. The input data for the computer program, however, were significantly refined by information obtained from experimental determination of the compressibility of Comp B filler and strain gage measurement of engraving forces under laboratory conditions. Results of subsequent instrumented firings were in good agreement with the refined analysis.

The distribution of tensile stresses for setback and engraving are shown graphically in Figures 14 and 15, respectively, for the most severe launch condition in each case, i.e., Zone 7 firing for maximum setback stresses and Zone 1 firing for maximum engraving stress.

As can be seen, the maximum tensile stress imposed by set back forces is a hoop stress of 23,000 psi through the full thickness of the projectile wall approximately 8.5 in. forward of the base. For engraving, the maximum tensile component of stress acts in the longitudinal direction and reaches a level of approximately 49,400 psi on the inner surface directly beneath the band seat.

An analysis of the forces developed during severe balloting (minimum bourrelet diameter and a worn gun tube) was also conducted using the method of Chu and Soechting[7]. Results indicated a maximum lateral force of approximately 28,000 lbs. at the bourrelet due to transverse motion of the projectile. This force was translated into stress by quasi-statically loading an instrumented projectile in the laboratory. A maximum tensile hoop stress of approximately 37,000 psi was found to occur on both the inner and outer surfaces of the ogive near the bourrelet.

Data obtained from the instrumented firings also show that the projectile is subjected to strain rates on the order of 1 to 10 in/in/sec during launch.

### Rough Handling Stresses

Drop tests of M107E1 projectiles instrumented with strain gages were used by Picatinny Arsenal to measure strains and rise times and thus provide the stress and strain rate information necessary for calculation of critical crack sizes for rough handling. On the basis of TECOM testing procedures, attention was focused on a drop height of

7 S. Chu and F. K. Soechting, "Transverse Motion of an Accelerating Projectile", Picatinny Arsenal Report, TR-4314, June 1972.

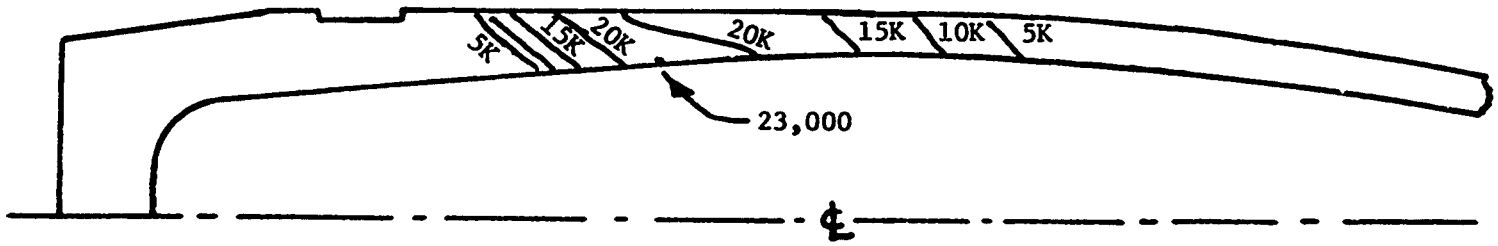


Figure 14. Tensile hoop stresses for launch, 155MM M107 projectile.

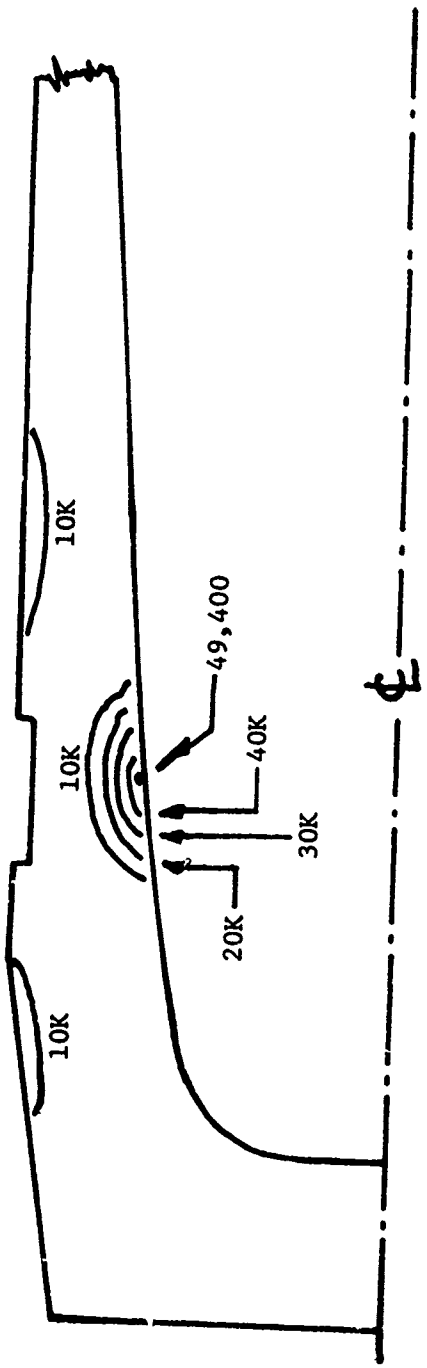


Figure 15. Tensile axial stresses for launch, 155MM M107 projectile.

7 feet and an impact surface of hardened steel backed by concrete. However, corresponding data were also obtained for impacts on a concrete surface without the steel facing.

The TECOM drop sequence for 155 mm projectiles specifies dropping in each of five orientations: (1) horizontal, (2) vertical (nose down), (3) vertical (base down), (4) oblique (nose down) and (5) oblique (base down). Of the five, the two oblique orientations were found to develop substantially higher stresses in the projectile than the other three. In the case of an oblique nose down drop, the most severe stresses result from a 30 degree impact angle and represent a tensile hoop stress very near the mouth of the projectile at the moment of initial impact. In the case of an oblique base down, the most severe stresses occur with a 45 degree impact angle. Unlike the oblique nose down impact, however, these peak stresses do not develop on initial impact, but rather, in a second impact which occurs when the projectile bounces, flips and reimpacts with it's nose angled approximately 30 to 45 degrees from horizontal. In this case, maximum stresses are also tensile hoop in nature and, again, located near the mouth of the projectile.

In the course of the investigation, two other impact conditions which resulted in relatively severe stresses were noted. These both involve a horizontally falling projectile landing on another projectile which is already lying on the impact surface. In one of these cases, the longitudinal axis of the falling projectile is oriented 90 degrees to the axis of the stationary projectile and the point of impact is at the center of gravity of each projectile (C.G. to C.G. drop). In the other case, the axes of the two projectiles are again at 90 degrees to each other, but the base of the falling projectile impacts the center of gravity of the stationary projectile. In the latter case, the nose of the falling projectile is tripped down onto the flat impact surface (tripping drop). These two projectile on projectile drop orientations, as well as the two oblique drops, are illustrated in Figure 16.

The maximum tensile components of stress determined for each of the four severe drop conditions cited above are shown in Table 8 for both steel and concrete impact surfaces, respectively. In order of severity, these are:

1. C. G. to C. G. - either steel or concrete - stresses above yield strength at point of contact.

2. Oblique (Base down) - steel - 99,400 psi tensile hoop at mouth.

3. Tripping - steel - 87,000 psi tensile hoop at mouth.

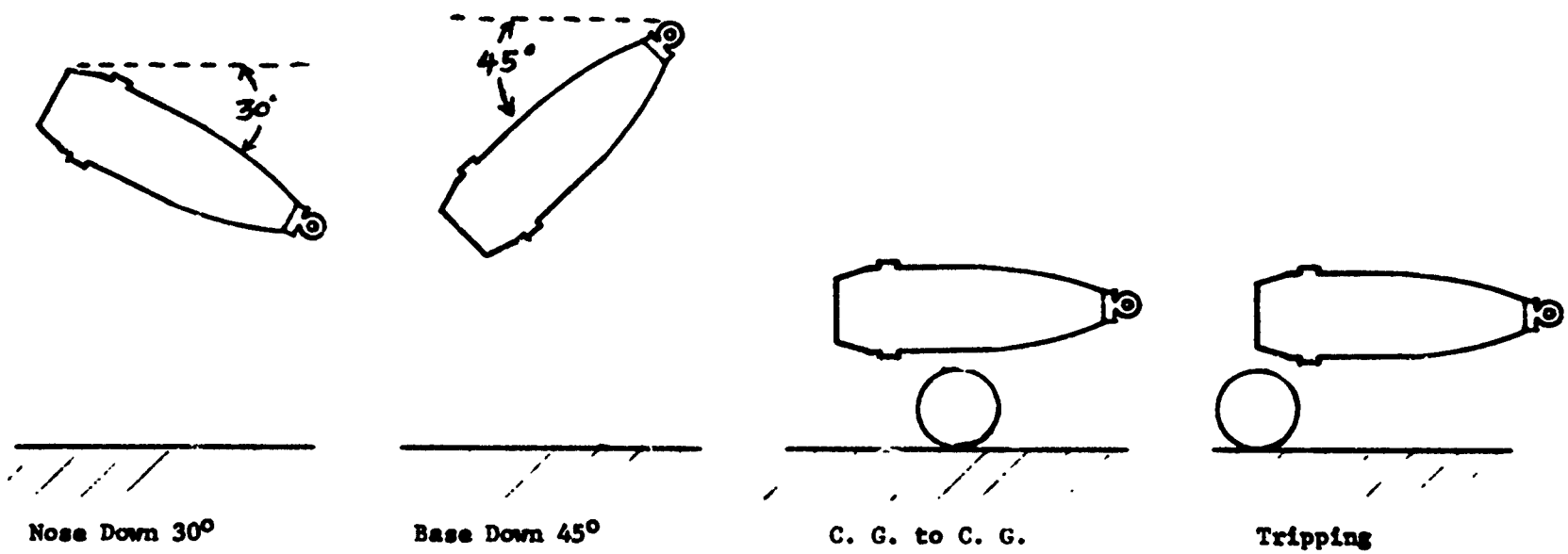


**Figure 16.** Sketch of the four most severe drop orientations

Table 8. Maximum Tensile Stresses Developed Under Various Drop Conditions

| Drop Condition | Impact Surface | Maximum Tensile Stresses (psi) | (Location) |
|---|---|---|---|
| Oblique - Nose Down | Steel | 64,000 | Mouth |
| Oblique - Nose Down | Concrete | 29,200 | Mouth |
| Oblique - Base Down | Steel | 99,400 | Mouth |
| Oblique - Base Down | Concrete | 46,200 | Mouth |
| C.G. to C.G. | Steel | >Yield Str | C.G. |
| C.G. to C.G. | Concrete | >Yield Str | C.G. |
| Tripping | Steel | 87,000 | Mouth |
| Tripping | Concrete | 62,000 | Mouth |

4. Oblique (Nose down) - steel - 64,000 tensile hoop at mouth.

5. Tripping - concrete - 62,000 psi tensile hoop at mouth.

6. Oblique (Base down) - concrete - 46,200 psi tensile hoop at mouth.

7. Oblique (Nose down) - concrete - 29,200 psi tensile hoop at mouth.

Strain rates determined from the instrumented drop tests were on the order of 5 to 50 in/in/sec.

## Critical Crack Sizes

The calc ated critical crack sizes for launch and rough handling are presented in Tables 9 and 10, respectively. The smallest critical flaw for launch is a 0.042 in. deep circumferential crack located on the inner wall directly beneath the band seat. This is related to the high axial tensile stresses developed during engraving under a low zone firing condition. For the severe drop (rough handling) conditions, where stresses are substantially higher than launch, critical flaw sizes are somewhat smaller.

For the sake of clarity, sketches depicting the locations of the critical flaws for launch and rough handling are shown in Figures 17 and 18.

## Drop Tests of Preflawed Projectiles

In order to provide a confirmation of the small critical flaw sizes calculated for rough handling, a number of M107E1 projectiles were intentionally flawed and subjected to the oblique base down drop test. This preflawing was accomplished by using an electric discharge machining (EDM) process to produce very narrow slots of controlled dimensions ranging in depth from 0.018 to 0.080 in. A single longitudinal slot was machined near the mouth of each projectile.

A replicating technique was used to determine the depths and notch acuity of the preflaws and a modified critical notch depth was calculated based on the determined acuity of the EDM slots, the fracture toughness of the projectile material and the anticipated drop stresses. This critical notch depth then served as the basis for predicting failure or survival in the drop tests.

Results of the preflawed projectile drop tests are summarized in Table 11. The data show that (1) the observed and predicted failures are in good agreement and (2) even though the as-machined notches are blunt relative to an actual crack, the critical flaw depth is still very

Table 9. Calculated Critical Crack Sizes for Launch - 155 mm, M107E1 Projectile

| Stress Source | $\sigma$ (ksi) | $K_{IC}$ (ksi$\sqrt{in}$) | $\sigma_{ys}$*1 (ksi) | ac (in.) |
|---|---|---|---|---|
| **Cold Conditioned (-65°F)** | | | | |
| Setback | 23.0 | 19.5 | 128.0 | 0.180 |
| Rotational | 19.0 | 19.5 | 128.0 | 0.239 |
| Engraving | 49.4 | 19.5 | 128.0 | 0.042 |
| Balloting | 37.0 | 19.5 | 128.0 | 0.076 |
| **Room Temperature (70°F)** | | | | |
| Setback | 23.0 | 24.1 | 100.0 | 0.244 |
| Rotational | 19.0 | 24.1 | 100.0 | 0.305 |
| Engraving | 49.4 | 24.1 | 100.0 | 0.064 |
| Balloting | 37.0 | 24.1 | 100.0 | 0.111 |
| **Elevated Temperature (200°F)** | | | | |
| Setback | 23.0 | 30.4 | 94.0 | 0.316 |
| Rotational | 19.0 | 30.4 | 94.0 | 0.368 |
| Engraving | 49.4 | 30.4 | 94.0 | 0.099 |
| Balloting | 37.0 | 30.4 | 94.0 | 0.167 |

*1 $\sigma_{ys}$ estimated at 20 $in/in.sec^{-1}$ (Heat A).

Table 10. Calculated Critical Crack Sizes for Selected Rough Handling (Drop) Conditions

| Drop Orientation | Impact Surface (1) | $\sigma$ ksi | $K_{IC}$ ksi$\sqrt{in}$ | $\bar{\sigma}$ ksi | $a_c$ (in) |
|---|---|---|---|---|---|
| | | **Cold Conditioned** | | | |
| Oblique-Nose Down | S | 64.0 | 19.5 | 128.0 | 0.025 |
| Oblique-Nose Down | C | 29.2 | 19.5 | 128.0 | 0.118 |
| Oblique-Base Down | S | 99.4 | 19.5 | 128.0 | 0.010 |
| Oblique-Base Down | C | 46.2 | 19.5 | 128.0 | 0.048 |
| C.G. to C.G. | B | >100 | 19.5 | 128.0 | <0.010 |
| Tripping | S | 87.0 | 19.5 | 128.0 | 0.013 |
| Tripping | C | 62.0 | 19.5 | 128.0 | 0.027 |
| | | **Room Temperature** | | | |
| Oblique-Nose Down | S | 64.0 | 24.1 | 100 | 0.038 |
| Oblique-Nose Down | C | 29.2 | 24.1 | 100 | 0.171 |
| Oblique-Base Down | S | 99.4 | 24.1 | 100 | 0.014 |
| Oblique-Base Down | C | 46.2 | 24.1 | 100 | 0.072 |
| C.G. to C.G. | B | >100 | 24.1 | 100 | <0.014 |
| Tripping | S | 87.0 | 24.1 | 100 | 0.019 |
| Tripping | C | 62.0 | 24.1 | 100 | 0.040 |
| | | **Elevated Temperature** | | | |
| Oblique-Nose Down | S | 64.0 | 30.4 | 94 | 0.059 |
| Oblique-Nose Down | C | 29.2 | 30.4 | 94 | 0.240 |
| Oblique-Base Down | S | 99.4 | 30.4 | 94 | 0.022 |
| Oblique-Base Down | C | 46.2 | 30.4 | 94 | 0.112 |
| C.G. to C.G. | B | >100 | 30.4 | 94 | <0.022 |
| Tripping | S | 87.0 | 30.4 | 94 | 0.029 |
| Tripping | C | 62.0 | 30.4 | 94 | 0.062 |

(1) S = Steel
C = Concrete
B = Both

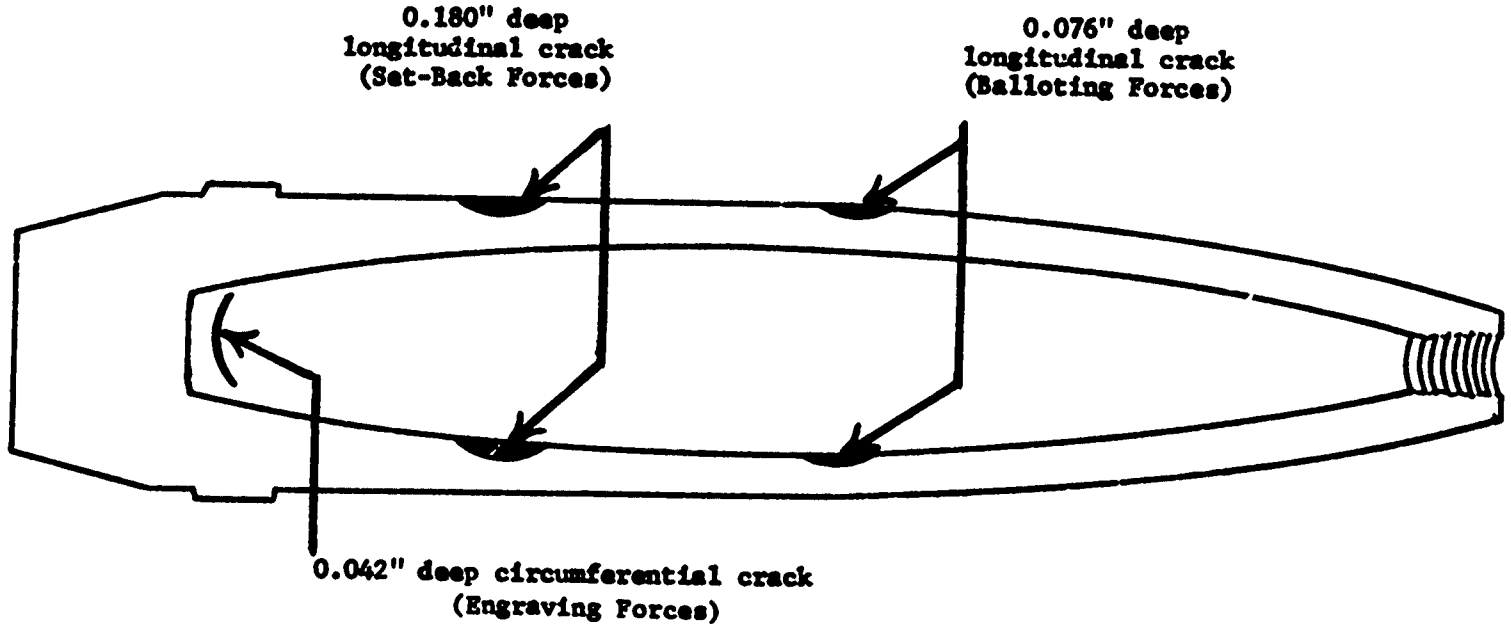


Figure 17. Schematic of minimum critical flaws for launch, M107E1 projectile, cold conditioned.

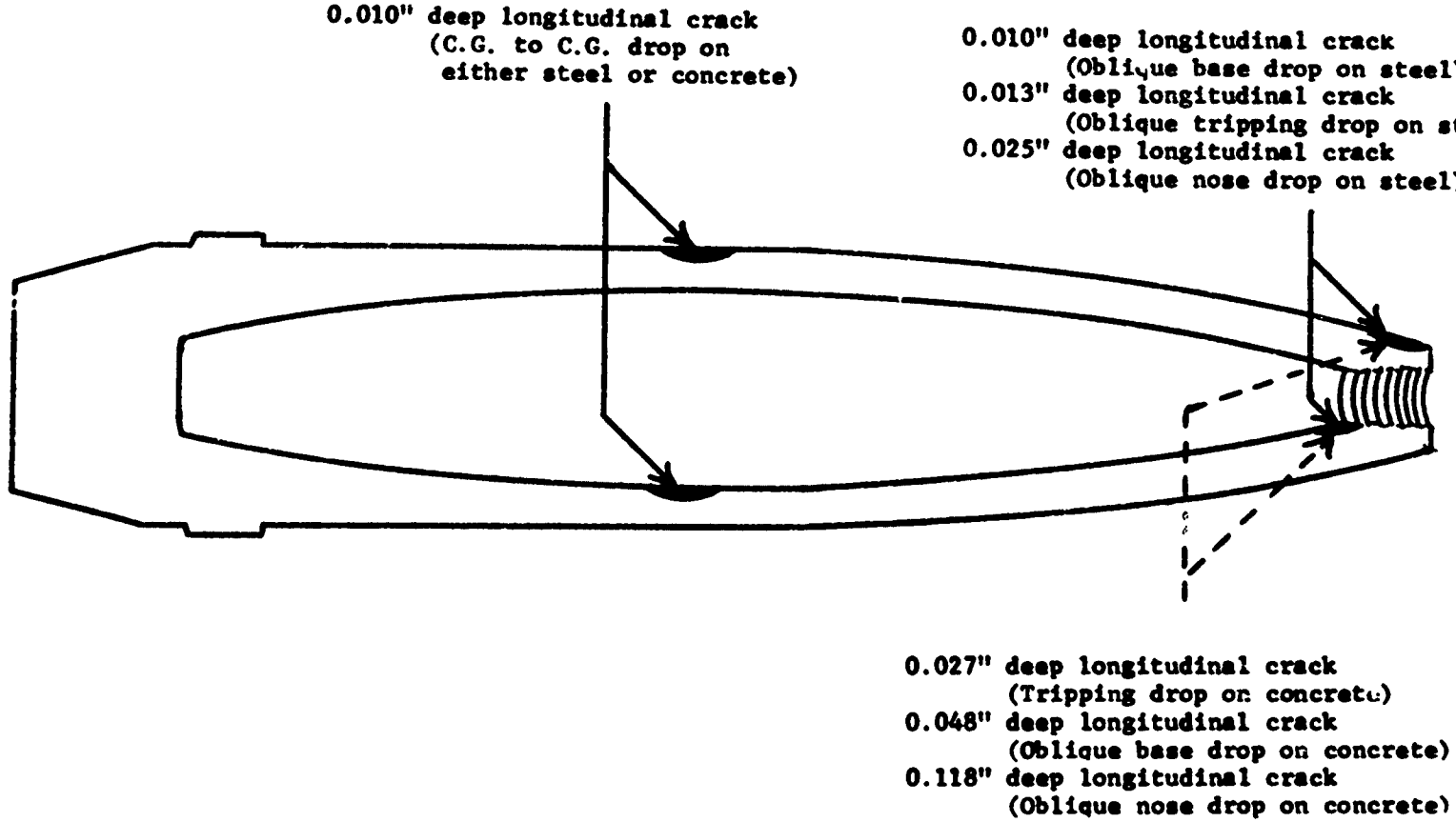


Figure 18. Schematic of minimum critical flaws for rough handling (drop), M107E1 projectile, cold conditioned

Table 11. Results of Base Down Drop Tests of Preflawed M107E1 Projectiles

| Defect Location | Test Temperature (°F) | Critical Sharp Crack Depth (in) | Critical Blunt Notch Defect (in) | Flaw * Depth (in) | Drop Results |
|---|---|---|---|---|---|
| Nose | 70 | 0.014 | 0.028 | 0.018 | Passed |
| Nose | 70 | 0.014 | 0.028 | 0.024 | Passed |
| Nose | 70 | 0.014 | 0.028 | 0.027 | Passed |
| Nose | 70 | 0.014 | 0.028 | 0.060 | Failed |
| Nose | 70 | 0.014 | 0.028 | 0.066 | Failed |
| Nose | 70 | 0.014 | 0.028 | 0.080 | Failed |
| Nose | -65 | 0.010 | 0.020 | 0.037 | Failed |

* Flaws were EDM notches near mouth of projectile

small (approximately 0.028" at room temperature and 0.020" at -65 degrees F). A photograph showing the large amount of crack extension from the small notches near the mouths of three projectiles which failed the test is shown in Figure 19.

## DISCUSSION

The major concerns of this study were to determine the minimum sizes of flaws which could critically affect the structural integrity of the M107E1 projectile as manufactured from isothermally transformed HF-1 steel, and to recommend, on the basis of those critical flaw sizes, whether it would be a safe projectile to manufacture and field.

The material characterization of the two heats of hot rolled plate and a third heat representing hot forged projectiles was sufficient to indicate that considerable variation in the properties of isothermally transformed HF-1 could be expected in large scale production. Since the chemistries of the three heats were essentially the same, the property variations observed can be attributed largely to (a) differences in the mechanical working processes which preceeded final isothermal transformation treatments; (b) minor differences in heat treating practices and (c) differences in grain size, all of which are common variations in industrial practice.

Despite these variations, the study, showed, unquestionably, that the plane strain fracture toughness of isothermally transformed HF-1 steel is significantly temperature sensitive over the range of temperatures within which an artillery projectile must function. Since fracture toughness was found to decrease steadily with decreasing temperature, critical flaw sizes must be based upon the properties of cold conditioned projectiles.

The studies also showed a tendency for fracture toughness to decrease slightly at intermediate strain rates before rising again at higher strain rates. Since the strain rates involved in launch and rough handling cover a rather wide range and cannot be precisely defined, calculation of critical flaw sizes must also be based on the minimum fracture toughness observed within the range of strain rates likely to be experienced.

On this basis, critical flaw sizes were calculated for the three major sources of stress in launch and for three of the four most severe conditions of rough handling. Calculations could not be made for the C.G. to C.G. drop condition because the stresses observed were above the yield strength of the projectile material. When significant yielding occurs, the elastic-plastic region can no longer be rigidly analyzed by linear elastic fracture mechanics in its present state of development. At best, an estimate can be made that a sharp flaw some



FIGURE 19. M107E1 projectiles with small EDM pre-flaws near the mouth which developed longitudinal splits in 7-foot drop tests involving oblique impact on flat steel surface

somewhat smaller than 0.010 in. deep could result in instability and lead to crack propagation. Fortunately, the small probability of precise C.G. to C.G. impact occurring in normal service and the extremely localized contact region involved make it very unlikely that any good quality projectile would contain such a defect at the precise location required.

Considering all six sources of stress for which critical flaw sizes were calculated, there are just two regions of the projectile in which extraordinary care would have to be taken to insure a sound product. These are: (1) the inner surface directly beneath the band seat where a circumferential crack as small as 0.042 in. deep could be critical and (2) the entire nose region of the projectile where longitudinal cracks as small as 0.010 in. deep could be critical.

Screening for cracks of the above size would require a highly sensitive and discriminating inspection technique. However, inspection for flaws of this size beneath the band seat would not necessarily represent an unsurmountable obstacle. In the first place, circumferential cracks are the least likely type to occur in that region under normal artillery projectile manufacturing methods, and, secondly, the critical region is so localized and well defined that stringent ultrasonic inspection of this restricted region would not be considered unreasonable.

The 0.010 in. deep critical flaw size near the mouth of the projectile, however, must be considered an extremely questionable restriction to place on the manufacture of an artillery projectile. To mass produce such an item and never have a flaw deeper than 0.010 in. is an unreasonable expectation and to inspect the entire nose region of a projectile for flaws of this size would be difficult and time consuming task. The difficulty is further compounded by the fact that most of this region is threaded on the inner surface to receive the lifting plug and fuze.

Because of the excessive processing controls which would be required to minimize the occurrence of these small flaws and the time consuming and costly inspection which would be required to insure the detection of all such flaws, the use of isothermally transformed HF-1 steel is not considered feasible for the high volume production of a safe and reliable M107E1 projectile.

## CONCLUSIONS

From the information developed under this study, it is concluded that:

1. The plane strain fracture toughness of isothermally transformed HF-1 steel is on the order of 25 KSI $\sqrt{\text{in.}}$ at room temperature

and 20 KSI $\sqrt{\text{in.}}$ at -65 degrees F.

2. The highest stresses imposed on an M107E1 projectile in its overall use environment are those encountered in rough handling (dropping). On impact from an oblique drop situation, these stresses are most severe in the nose of the projectile and reach values approaching 100,000 psi.

3. Critical flaw sizes for launch are on the order of 0.075 in. deep in the sidewall and 0.040 in. deep under the rotating band.

4. The smallest critical flaw size associated with rough handling is on the order of 0.010 in. deep for oblique impacts in a 7-foot drop test.

## RECOMMENDATIONS

In consideration of these findings, the following recommendations are made:

1. Isothermally transformed HF-1 steel should not be considered for use in an artillery projectile of the M107 configuration.

2. Alternate materials such as quenched and tempered HF-1, 9260 and 1340 steels should be studied with respect to their flaw tolerance and fragmentation performance for possible use as a cost effective material for an improved fragmentation projectile of the M107 configuration.

3. Critical flaw size determinations should be carried out in the early selection stages of all future projectile development programs involving an advanced fragmentation material. These determiations must consider both launch and rough handling (drop) environments.

4. Assuming that the TECOM drop test requirements provide a valid representation of the severity of actual field handling situations, consideration should be given to devising means of reducing projectile stresses under drop conditions. Such consideration should include both the design of the projectile itself, and the possible use of protective (impact absorbing) packaging at the nose region of the projectile.